Optimized Vehicles Dimensioning, Dispatching and Charging Schemes for Multi-class Autonomous Electric Mobility On-demand Systems

A Thesis

Presented in Partial Fulfillment of the Requirements for the

Degree of Master of Science

with a

Major in Electrical and Computer Engineering

in the

College of Graduate Studies

University of Idaho

by

Syrine Belakaria

Major Professor: Sameh Sorour, Ph.D.

Committee Members: Brian Johnson, Ph.D., P.E.; Ahmed Abdel-Rahim, Ph.D., P.E.

Department Administrator: Joseph Law, Ph.D., P.E.

August 2018

Authorization to Submit Thesis

This thesis of Syrine Belakaria, submitted for the degree of Master of Science with a major in Electrical and Computer Engineering and titled "Optimized Vehicles Dimensioning, Dispatching and Charging Schemes for Multi-class Autonomous Electric Mobility On-demand Systems," has been reviewed in final form. Permission, as indicated by the signatures and dates given below, is now granted to submit final copies to the College of Graduate Studies for approval.

Major Professor: _____Date_____
Sameh Sorour, Ph.D.

Committee Members: _____Date_____
Brian Johnson, Ph.D., P.E.

_____Date_____
Ahmed Abdel-Rahim, Ph.D., P.E.

Department Administrator: _____Date_____
Joseph Law, Ph.D., P.E.

Abstract

Despite the significant advances in vehicle automation and electrification, the next-decade aspirations for massive deployments of autonomous electric mobility on demand (AEMoD) services in big cities are still threatened by two major bottlenecks, namely the communication/computation and charging delays. In order to target the communication/computation delays, the thesis suggests the exploitation of fog-based architectures for localized AEMoD system operations. These emerging architectures are soon-to-become widely used, allowing for all localized operational decisions to be made with very low latency by fog controllers located close to the end applications (e.g., each city zone for AEMoD systems). As for the charging delays, an optimized multi-class charging and dispatching management model, with partial charging option for AEMoD vehicles, is developed for each of these zones as a queuing system. The stability conditions of this model and the optimal number of classes are then derived. Decisions on the proportions of each class vehicles to partially/fully charge or directly serve customers are optimized to minimize the maximum and average system response times. The study of the model covered also finding the optimal vehicle dimensioning for each zone in order to guarantee a bounded need of vehicles with a bounded response time. This study aimed also to resolve a clear and unrealistic limitation in the first proposed model, namely the matched charge-to-trip only service, by enabling sub-class service; i.e., allowing vehicles to serve customer classes with trips needing less charge. A queuing model representing the new multi-class management scheme is introduced. Its stability conditions are then derived. Decisions on the proportions of each class's vehicles to charge and to partially/fully charge, or directly serve customers with sub-class service are then optimized in order to minimize the maximum response time of the system. Both of the proposed models were simulated and results show the merits of our proposed models and optimized decision schemes compared to several non optimized schemes.

Keywords: Autonomous Mobility On-Demand; Electric Vehicles; Queuing Systems.

Acknowledgements

The outcome of my work has required a lot of guidance and assistance and inspiration from many people to whom I would like to express special appreciation:

First and foremost, I heartily thank Dr. Sameh Sorour, my major professor, who believed in my potential and gave me the opportunity to gain this valuable experience. Without his assistance and dedicated involvement, this work would have never been accomplished. I am thankful and indebted to him for sharing not only expertise and knowledge but also sincere and valuable guidance and encouragement during my master degree.

I owe my profound gratitude and special thanks to Dr. Ahmed Abdel-rahim, the director of Niatt who also participated in this work and supported it.

A deep appreciation goes to my professors: Dr. Brian Johnson, who was an amazing teacher and a very supportive professor, Dr. Ting-Yen Shih and Dr. John Chiasson from whom I got my first teaching experience. I want to thank them for their timely encouragement all along the completion of my work.

This work has been funded by the U.S. Department of Transportation's University Transportation Center program, Grant # 69A3551747110 through the Pacific Northwest Regional University Transportation Center (PacTrans). I would like to thank PacTrans for their support. It was also supported by the National Institute for Advanced Transportation Technologies, University of Idaho, Moscow, Idaho, U.S.A . I would like to thank all who contribute to this study from both funding agencies.

A special thank goes to my collaborator Mustafa Ammous and my friends Taha Belkhouja and Maha Bouhadida who have been available to support me every day of my work despite the constraints.

Finally, I admit that words may not be able to express my gratitude to my family for contributing in all the ways to my success. I want to thank them for their unconditional support during not only my Master but my whole path.

Dedication

In the Name of God Almighty, Most Gracious, Most Merciful,I dedicate this work to

My father who has always believed in me

My mother for all the support and the sacrifices she made on my behalf. Your prayers for me was what sustained me this far.

Taha, my fiancee, for being there every day, for enlightening my path in, for all the unforgettable memories we made together, for the love and care you provided me.

Amira, my sister, who stood by my side in the hardest moment and believed in me even when no one else did. My sisters and brother Imen, Ines, Soumaya and Amine, who were always there for me.

My nieces for the joy the entered to my life and heart.

Maha for her sincere friendship, for her trust and faith, for standing by my side in joy and sorrow, for the beautiful moments we shared together and marked my life.

All my dearest friends and family, for their continuous encouragement.

Table of Contents

List of Tables

List of Figures

CHAPTER 1

Introduction

This thesis includes: in the second chapter, a paper [1] that had been published in *in Proc. of IEEE Vehicular Technology Conference (VTC'17-Fall)*, Toronto, ON, Canada, September 2017. and in the third chapter another paper [3] that was accepted for publication in *IEEE International Communication Conference (ICC)*, 2018. Both of those paper were co-authored by Mustafa Ammous, Dr. Sameh Sorour and Dr. Ahmed Abdel-Rahim.

1.1 Motivation

Urban transportation systems are experiencing tremendous challenges nowadays due to the exploding demand on private vehicle ownership, which result in dramatic increases in road congestion, parking demand [5], increased travel times [6], and carbon footprint [7] [8]. This clearly calls for revolutionary solutions to sustain the future private mobility. Mobility on-demand (MoD) services were successful in providing a partial solution to the increased private vehicle ownership problem [9], by providing one-way vehicle sharing between dedicated pick-up and drop-off locations for a monthly subscription fee, and with no worries for vehicle insurance and maintenance costs. The electrification of such MoD vehicles can also gradually reduce the carbon footprint problem. However, the need to make extra trips for picking-up, after dropping-off, and occasionally for fueling /charging these MoD vehicle has significantly affected the convenience of this solution and reduced its effect in solving urban traffic problems.

Nonetheless, an expected game-changer for the success of these services is the significant advances in vehicle automation and wireless connectivity. With more than 10 million self-driving vehicles expected to be on the road by 2020 [10], and the vision of governments and automakers to inject more wireless connectivity, and coordinated optimization on city roads, it is strongly forecasted that private vehicle ownership will significantly decline by

2025, as individuals' private mobility will further depend on the concept of Autonomous Electric MoD (AEMoD) [11] [12]. Indeed, AEMoD systems will preserve the benefits of current MoD systems, but relieve customers from their inconveniences, including picking-up and dropping-off vehicles at dedicated locations, parking hassle/delays, and fueling/charging detours. Indeed, the self-driving feature in these vehicles will allow them to navigate to customers' locations for pick-up, locate spots for parking after customer drop-off, and self-drive to fuel/charging stations between customer trips when needed. Moreover, it will provide them with added time of in-vehicle work and leisure. In short, AEMoD systems will enable customers to simply press some buttons on an app to promptly get an autonomous electric vehicle to transport them door-to-door, with no pick-up/drop-off and driving responsibilities, no dedicated parking needs, no carbon emission, no vehicle insurance and maintenance costs, and extra in-vehicle work/leisure times. With all of these ecological, economical, and customer-oriented qualities, AEMoD systems are highly expected to significantly prevail in attracting millions of subscribers across the world and in providing on-demand and hassle-free private urban mobility.

Despite the great aspirations for wide AEMoD service deployments by early-to-mid next decade, the timeliness of such service (i.e., promptness in providing a ready vehicle to each requesting customer with minimum or bounded delays), and thus its entire success, is threatened by two major bottlenecks. First, the expected massive demand of AEMoD services will result in excessive, if not prohibitive, computational and communication delays if cloud based approaches are employed for the micro-operation (e.g., collecting requests, and optimizing dispatching and charging decisions) of such systems. Moreover, the typical full-battery charging rates of electric vehicles will not be able to cope with the gigantic numbers of vehicles involved in these systems, thus resulting in instabilities and unbounded customer delays.

1.2 Related Work

Mobility on demand services were studied from several perspectives since the performance of these systems depends on many factors, such as the charging resources, customers satisfaction, waiting time, etc. Recent works have addressed important problems in AMoD systems by building different operation models for them. In [14], the authors proposed two different models: a distributed queuing model in which they spatially averaged the customers queues into one queue, and a lumped model that exploits the theory of Jackson networks. These models were employed to analyze the re-balancing between the stations. In [18] a lumped spatial-queuing model was proposed. Several non-practical assumption were made in order to treat the problem as a Jackson Network. [17] casted an AMoD system into a closed multi-class BCMP queuing network model, and solved the routing problem for rebalancing vehicles on congested roads. Many key factors were not considered in this work in order to simplify the mathematical resolution. None of these papers considered the computational architecture for massive demands on such services, the vehicle electrification, and the influence of charging limitations on its stability.

In [15], the paper presents a model predictive control (MPC) approach to optimize the dispatching and scheduling of the vehicles in AMoD systems. It is valuable to apply the MPC algorithms to minimize the future waiting time of customers, but the optimization of the proposed system was done without or with very simplistic consideration of the AMoD vehicle electrification. The MPC technique was also used in more recent works like [21], where a finite-horizon dynamic programming algorithm was proposed to provide optimal schedules for plug-in electric vehicles (PEV) charging given statistical information on their future charging demands. The focus was more on reducing the algorithm complexity compared to similar algorithms proposed in [24] and [25].

In [26] [27] [28], the authors designed an artificial neural network to predict the quality of service of an MoD system for campus demand utilizing a small number of vehicles. Com-

bined predictive positioning and ridesharing approaches were shown to achieve a valuable MOD fleet management performance but this performance does not stand for a city scale.
In [19], the authors addressed the vehicle dispatching problem based on distances separating vehicles from customers. They employed a combination of the Euclidean bipartite matching problem and random permutation theory to minimize the trip cost, but without considering the charging limitation.
Charging AEMoD vehicles was also studied from different perspectives. Some works [20] [22] proposed optimization models to reduce the cost in term of power and energy. [20] provided a valuable analysis to an approximate dynamic programming system with feedback-based optimization for the charging process. In [22], a time variant cost optimization was proposed for charging at Photovoltaics charging stations. In [23], the involvement of smart grids for energy cost optimization were not only studied by closed loop and open loop methods, but also using artificial intelligence techniques. These techniques allowed to introduce several agents and complex models, like considering the vehicles themselves as sources of energy that can contribute to the grid. AI might have valuable outcomes but the cost and complexity of deploying these methods are high. Our work is different from [20] [22] [23] since it aims to optimize the system response/waiting times for customer satisfaction.

1.3 Our Contributions

In this thesis, we target the two timeliness limitations hindering the success of AEMoD systems, namely the communication/computation delays and possible system instability due to the charging process. To resolve the first limitation, we suggest the exploitation of the new and trendy *fog-based networking and computing architectures* [36] [29] [13]. While long propagation delays remain a key drawback for centralized Cloud Computing, MEC with the proximate access is widely agreed to be a key technology for realizing various application for next-generation Internet with millisecond-scale reaction time [32]. The privileges brought by this technique will allow handling vehicular networks [37] in need for instantaneous decision

making applications such autonomous mobility [40]. Consequently, they can also be involved in handling AEMoD system operations in a distributed way. This approach will push the operational decision load close to end customers in each city zone, thus reducing the computational complexity and communication delays. Luckily, this architecture perfectly fits the nature of many AEMoD fleet operations that are mostly local, such as dispatching and charging. Indeed, AEMoD vehicles will be usually directed to pick up customers close to their locations and charge at near-by charging stations. This thus makes the fog-based architectures well-suited localized solutions to guarantee low communication and computation latencies for such local management operations.

Having this component resolved by the aforementioned soon-to-be-deployed technologies, the thesis focuses on resolving the second timeliness bottlneck by proposing a multi-class dispatching and charging approach in each service zone. The proposed approach classifies its incoming vehicles according to their state-of-charge (SoC) and smartly manages their charging options according to the available charging resources in this zone. This management is done through introducing the option of no or partial charging for vehicles with non-depleted batteries, and enabling the full charging option only to vehicles will fully depleted batteries. This multi-class system also allocates these vehicles to the different classes of customers according to the suitableness of the vehicles SoC for the customer trip distance. The thesis also proposes the enhancement of this model by introducing the ability to serve customers of any class for which a vehicles has enough amount of charge.

Given these novel system operation architecture, the questions now becomes: *What is the optimal proportion of vehicles from each class to dispatch (i.e., no charging) or partially/fully charge, to both maintain charging stability and minimize the maximum or average* response times *of the system? What is the system dimension and vehicles in-flow that can satisfy the demand of customers with respect to a limited average waiting time? What are the optimal proportions of vehicles dispatching to different sub-classes that will allow having an enhanced system?* To address these questions, in the Second chapter, a queuing model representing

the proposed fog-based multi-class charging and dispatching scheme is first introduced. An analytical and numerical studies of the proposed system are done in order to minimize the maximum and average system *response times* and show the merits of the model compared to other non-optimized schemes. In the third chapter, an optimization of the vehicles inflow rates is conducted analytically and simulations that shows the the performance of the system are presented. Finally in the fourth chapter, an enhanced system model, that solves some unrealistic boundaries of the first proposed system, is proposed. an optimization of the maximum expected response time showed that the enhancement brought to this model allows it to out perform the first model and other non optimized policies.

CHAPTER 2

Fog-Based Multi-Class Dispatching and Charging for Autonomous Electric Mobility On-Demand

[1] "A Multi-Class Dispatching and Charging Scheme for Autonomous Electric Mobility On-Demand," *in Proc. of IEEE Vehicular Technology Conference (VTC'17-Fall)*, Toronto, ON, Canada, September 2017.

Introduction

In this chapter, We suggest the exploitation of fog-based architectures for localized AEMoD system operations. This architecture is defined justified by multiple references that explains the income and advantages brought by it. Later an optimized multi-class charging and dispatching queuing model, with partial charging option for AEMoD vehicles, is developed for each of these zones. The stability conditions of this model and the number of classes that fit the charging capabilities of the service zone are then derived. Decisions on the proportions of each class vehicles to partially/fully charge, or directly serve customers are then optimized to minimize the maximum and average system *response times*. The maximum and average *response time* minimization problems are formulated as stochastic linear and convex optimization problems, respectively, and optimal decisions are analytically derived for each problem using Lagrangian analysis. Finally, the merits of our proposed optimized decision scheme are tested and compared to both the always-charge and the equal split schemes. Furthermore, the comparison of the maximum and average response time minimization results shows a very low variance in performance, which suggests using the linear programming solution for lower complexity.

2.1 Proposed System Model

2.1.1 Fog-based Architecture

Fog-based architectures have recently emerged as novel distributed edge computing architectures to both mitigate the communication and computational burdens on backhaul networks and cloud servers, respectively, and reduce the delays for system analytics and decision making. These architectures push computational resources close to the end entities, thus providing them with low complexity and latency analytics and optimization solutions through local communications with these resources. The concept of MEC was firstly proposed by the European Telecommunications Standard Institute (ETSI) in 2014, and was defined as a new platform that "provides IT and mobile cloud computing capabilities (MCC) within the Radio Access Network (RAN) in close proximity to mobile subscribers" [30]. This led to the emergence of a new research area called Fog Computing and Networking [31]. It is widely agreed and proved that the MEC will solve the delays disadvantages in mobile cloud computing (MCC) [32]. [29] provides a clear comparison that shows the benefits brought by MEC compared to MCC. The supportable latency for MEC is less than ten milliseconds while being larger than 100 milliseconds for MCC. It was also shown that the fog computing has $10^2 - 10^4$ times higher computation capabilities than the minimum requirement for heavy computational complexity applications, like gaming [33], autonomous driving, and instantaneous decision making applications [30] [35]. Moreover, with its small distance to end users, fog computing provides a reduced backhaul usage, thus alleviating congestions [34] [39]. In addition to the previous previlages, fog-based architectures are highly energy efficient with respect to supporting computation offloading, and are thus considered as green technologies [36] [40] [38].

As clearly mentioned earlier, our proposal to employ a fog-based architecture for AEMoD systems is justified by the fact that many of the AEMoD operations (e.g., dispatching and charging) are localized with very high demand and instantaneous decision-making needs.

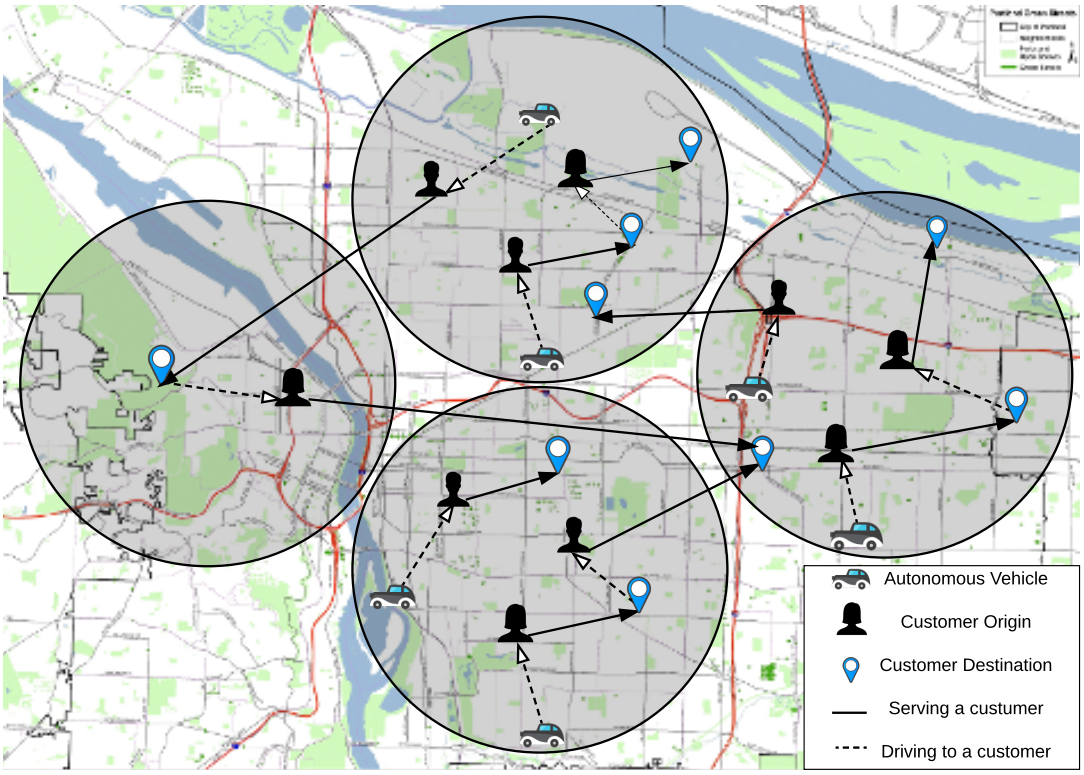

Figure 2.1: Fog-based architecture for AEMoD system operation

Indeed, vehicles located in any city zone are the ones that can reach the customers in that zone within a limited time frame. They will also charge in near-by charging points within the zone. Fig.2.1 illustrates a candidate fog-based architecture that can support real-time micro-operational decisions (e.g, dispatching and charging) for AEMoD systems with extremely low computation and communications delays. The fog controller in each service zone is responsible of collecting information about customer requests, vehicle in-flow to the service zone, their state-of-charge (SoC), and the available full-battery charging rates in the service zone. Given the collected information, it can promptly make dispatching, and charging decisions for these vehicles in a timely manner.

2.1.2 Multi-Class Dispatching and Charging Model

To guarantee the stability and timeliness of future AEMoD systems given the relatively limited charging resources compared to demand volumes, it is very critical to answer two important operational questions: (1) How to cope with the available charging capabilities of each service zone given the large number of system vehicles? (2) How to smartly manage the dispatching and charging options of different SoC vehicles, given the customers' needs and zone resources, in order to minimize the maximum and/or average system response time. By the system *response time*, we mean the time elapsed between the instant when an arbitrary customer requests a vehicle, and the instant when a vehicle starts moving from its parking or charging spot towards this customer.

Motivated by the fact that different customers can be classified in ascending order of their required trip distances (and thus the SoC needed in their allocated vehicles), this thesis proposes to address the two above questions by introducing a multi-class dispatching and charging scheme for AEMoD vehicles, with options of partial charging for vehicles with non-depleted batteries. Arriving vehicles in each service zone are subdivided into different classes in ascending order of their SoC corresponding to the different customer classes. Different proportions of each class vehicles will be then prompted by the fog controller to either wait (without charging) for dispatching to its corresponding customer class (i.e., customers whose trips will require the SoC range of this class vehicles) with or partially charge to serve the subsequent customer class. Vehicles arriving with depleted batteries will be allowed to either partially or fully charge to serve the first or last class customers, respectively. Clearly, the larger the number of classes, the smaller the SoC increase required for a vehicle to move from one class to the next, the smaller the charging time needed to make this transition, the less the burden/requirements on the zone charging resources. On the other hand, given a fixed in-flow rate of vehicles to each city zone, more vehicle/customer classes means less available in-flow vehicles to each customer class, which may result in longer service delays and even

instabilities in their waiting queues.

Given this proposed multi-class system solution, the first and second above questions can then be re-phrased as: (1) What is the minimum number of classes that can fit the available charging resources in a given city zone? (2) What is the optimal proportion of vehicles from each class to dispatch or partially/fully charge to both maintain the overall system stability and minimize the maximum and/or average *response time* of the system? To rigorously address these questions, we will first model our proposed multi-class charging and dispatching solution as a queuing model and introduce its parameters in the next section.

2.1.3 Queuing Model and System Parameters

We consider one service zone controlled by a fog controller connected to: (1) the service request apps of customers in the zone; (2) the AEMoD vehicles; (3) C rapid charging points distributed in the service zone and designed for short-term partial charging; and (4) one spacious rapid charging station designed for long-term full charging. AEMoD vehicles enter the service in this zone after dropping off their latest customers in it. Their detection as free vehicles by the zone's controller can thus be modeled as a Poisson process with rate λ_v. Customers request service from the system according to a Poisson process. Both customers and vehicles are classified into n classes based on an ascending order of their required trip distance and the corresponding SoC to cover this distance, respectively. From the thinning property of Poisson processes, the arrival process of Class i customers and vehicles, $i \in \{0, \ldots, n\}$, are both independent Poisson processes with rates $\lambda_c^{(i)}$ and $\lambda_v p_i$, where p_i is the probability that the SoC of an arriving vehicle to the system belongs to Class i. Note that p_0 is the probability that a vehicle arrive with a depleted battery, and is thus not able to serve immediately. Consequently, $\lambda_c^{(0)} = 0$ as no customer will request a vehicle that cannot travel any distance. On the other hand, p_n is also equal to 0, because no vehicle can arrive to the system fully charged as it has just finished a prior trip.

Upon arrival, each vehicle of Class i, $i \in \{1, \ldots, n-1\}$, will park anywhere in the

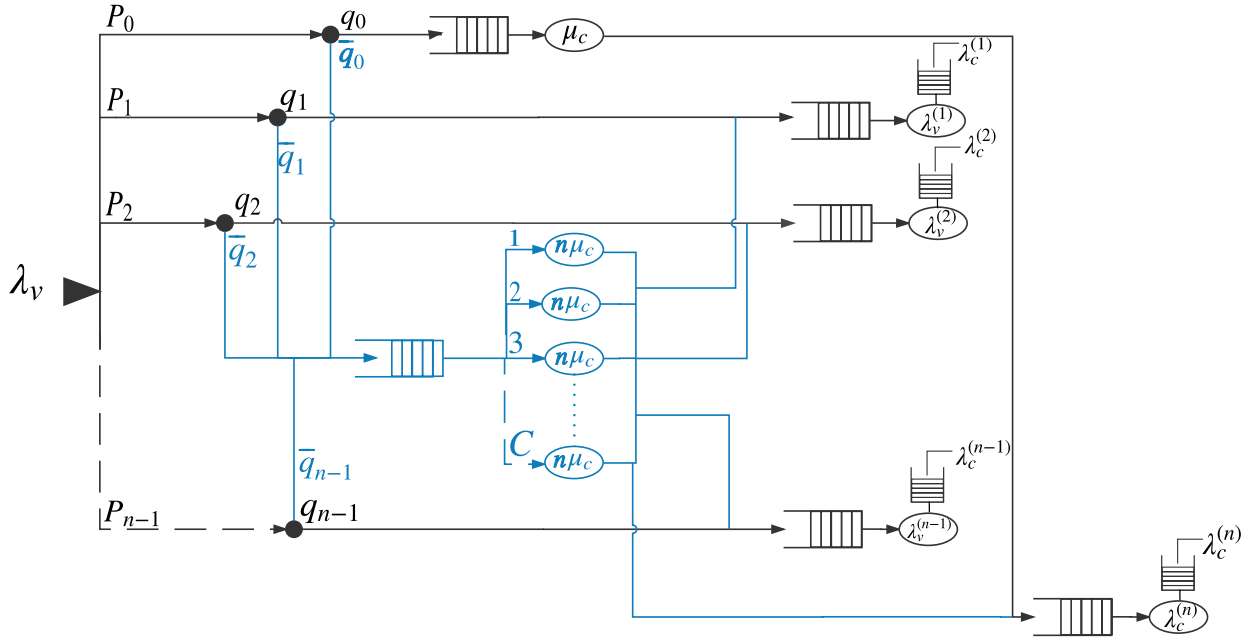

Figure 2.2: Joint dispatching and partially/fully charging model, abstracting an AEMoD system in one service zone.

zone until it is called by the fog controller to either: (1) serve a customer from Class i with probability q_i; or (2) partially charge up to the SoC of Class $i+1$ at any of the C charging points (whenever any of them becomes free), with probability $\bar{q}_i = 1 - q_i$, before parking again in waiting to serve a customer from Class $i+1$. As for Class 0 vehicles that are incapable of serving before charging, they will be directed to either fully charge at the central charging station with probability q_0, or partially charge at one of C charging points with probability $\bar{q}_0 = 1 - q_0$. In the former and latter cases, the vehicle after charging will wait to serve customers of Class n and 1, respectively.

The full charging time of a vehicle with a depleted battery is assumed to be exponentially distributed with rate μ_c. Given uniform SoC quantization among the n vehicle classes, the partial charging time can then be modeled as an exponential random variable with rate $n\mu_c$. Note that the larger rate of the partial charging process is not due to a speed-up in the charging process but rather due to the reduced time of partially charging. The use of exponentially distributed charging times for charging electric vehicles has been widely used

Table 2.1: List of System and Decision Parameters

Variables	Definition
λ_v	Total arrival rate of vehicles
p_i	Probability of arrival of a vehicle from Class i
q_0	Probability that a battery-depleted vehicle partially charges
$\overline{q}_0$	Probability that a battery-depleted vehicle fully charges
$q_i, i \neq 0$	Probability that a vehicle in Class i is directly dispatched
$\overline{q}_i, i \neq 0$	Probability that a vehicle in Class i partially charges
μ_c	Service rate of fully charging a battery-depleted vehicle
$\lambda_v^{(i)}$	Arrival rate of vehicles of Class i
$\lambda_c^{(i)}$	Arrival rate of customers served by Class i's vehicles
C	No. of distributed charging points in the service zone of the fog controller

in the literature [16, 17] to model the randomness in the charging duration of the different battery sizes. The customers belonging to Class i, arriving at rate $\lambda_c^{(i)}$, will be served at a rate of $\lambda_v^{(i)}$, which includes the arrival rate of vehicles that: (1) arrived to the zone with a SoC belonging to Class i and were directed to wait to serve Class i customers; or (2) arrived to the zone with a SoC belonging to Class $i-1$ and were directed to partially charge to be able to serve Class i customers.

Given the above description and modeling of variables, the entire zone dynamics can thus be modeled by the queuing system depicted in Fig.2.2. This system includes n M/M/1 queues for the n classes of customer service, one M/M/1 queue for the charging station, and one M/M/C queue representing the partial charging process at the C charging points.

Having defined the queuing model for the proposed multi-class dispatching and charging system in a city zone, the rest of the chapter will focus on addressing the two questions in Section 2.1.2. We will first determine the stability conditions of the system and minimum number of required classes to cope with the charging resources in any arbitrary city zone in Section 2.2. The maximum and average response time minimization problems will be then formulated and analytically solved in Sections 2.3 and 2.4, respectively.

2.2 System stability conditions

In this section, we first deduce the stability conditions of our proposed multi-class dispatching and charging system, using the basic laws of queuing theory. We will then derive an expression for the lower bound on the number n of needed classes that fit the charging capabilities of any arbitrary service zone. Each of the n classes of customers are served by a separate queue of vehicles, with $\lambda_v^{(i)}$ being the arrival rate of the vehicles that are available to serve the customers of the i-th class. Consequently, it is the service rate of the customers i-th arrival queues. We can thus deduce from Fig. 2.2 and the system model in the previous section that:

$$\begin{aligned} \lambda_v^{(i)} &= \lambda_v \left(p_{i-1}\overline{q}_{i-1} + p_i q_i\right) \qquad\qquad i = 1, \ldots, n-1 \\ \lambda_v^{(n)} &= \lambda_v \left(p_{n-1}\overline{q}_{n-1} + p_0 q_0\right) \end{aligned} \tag{2.1}$$

Since we know that $\overline{q}_i + q_i = 1$, we substitute $\overline{q}_i$ by $1 - q_i$ in order to have a system with n variables

$$\begin{aligned} \lambda_v^{(i)} &= \lambda_v \left(p_{i-1} - p_{i-1}q_{i-1} + p_i q_i\right) \qquad i = 1, \ldots, n-1 \\ \lambda_v^{(n)} &= \lambda_v \left(p_{n-1} - p_{n-1}q_{n-1} + p_0 q_0\right) \end{aligned} \tag{2.2}$$

From the well-known stability condition of an M/M/1 queue [42] [43], we have:

$$\lambda_v^{(i)} > \lambda_c^{(i)} \qquad\qquad i = 1, \ldots, n \tag{2.3}$$

Before reaching the customer service queues, the vehicles will go through a decision step on whether to go to these queues immediately or partially/fully charge. The stability of the charging queues should be guaranteed in order to ensure the global stability of the entire system at the steady state. From the model described in the previous section, and by the well-known stability conditions of M/M/C and M/M/1 queues [42] [43], we have the following stability constraints on the C charging points and central charging station queues,

respectively:

$$\begin{aligned} &\sum_{i=0}^{n-1} \lambda_v \left(p_i - p_i q_i\right) < C \left(n\mu_c\right) \\ &\lambda_v p_0 q_0 < \mu_c \end{aligned} \tag{2.4}$$

The following lemma illustrates the lower bound on the average in-flow rate of vehicles for a given service zone given its rate of customer demands on AEMoD services.

Lemma 1. *For the entire system stability, the in-flow rate of vehicles to a given service zone should be strictly more than the total arrival rate of customers belonging to all the classes. In other words,*

$$\sum_{i=1}^{n} \lambda_c^{(i)} < \lambda_v \tag{2.5}$$

Proof. The proof of Lemma 1 is in Appendix A. □

Furthermore, the following lemma establishes a lower bound on the number of classes n, given the arrival rate of the vehicles λ_v, the full charging rate μ_c, and the number C of partial charging points.

Lemma 2. *To guarantee the stability of the charging queues, the number of classes n is the system must obey the following inequality:*

$$n > \frac{\lambda_v}{C\mu_c} - \frac{1}{C} \tag{2.6}$$

Proof. The proof of Lemma 2 is in Appendix B. □

2.3 Maximum Response Time Optimization

The goal of this section is to minimize the maximum expected response time across all system's classes.

2.3.1 Problem Formulation

The expected response time of any class is defined as the expected duration between any customer putting a request until a vehicle is dispatched to serve him/her. From the basic M/M/1 queue analysis of the i-th customer class, the expression of this expected response time for the i-th class can be expressed as:

$$\frac{1}{\lambda_v^{(i)} - \lambda_c^{(i)}} \qquad i = 1, \ldots, n \tag{2.7}$$

Consequently, the maximum of the expected response times across all n classes of the system can be expressed as:

$$\max_{i \in \{1,\ldots,n\}} \left\{ \frac{1}{\lambda_v^{(i)} - \lambda_c^{(i)}} \right\} \tag{2.8}$$

It is obvious that the system's class having the maximum expected response time is the one that have the minimum expected response rate. In other words, we have:

$$\arg \max_{i \in \{1,\ldots,n\}} \left\{ \frac{1}{\lambda_v^{(i)} - \lambda_c^{(i)}} \right\} = \arg \min_{i \in \{1,\ldots,n\}} \left\{ \lambda_v^{(i)} - \lambda_c^{(i)} \right\} \tag{2.9}$$

Consequently, minimizing the maximum expected response time across all classes is equivalent to maximizing their minimum expected response rate. Using the epigraph form [41] of

the latter problem, we get the following stochastic optimization problem:

$$\max_{q_0,q_1,\ldots,q_{n-1}} \quad R \tag{2.10a}$$

s.t.

$$\lambda_v \left(p_{i-1} - p_{i-1}q_{i-1} + p_i q_i\right) - \lambda_c^{(i)} \geq R,\ i = 1, \ldots, n-1 \tag{2.10b}$$

$$\lambda_v \left(p_{n-1} - p_{n-1}q_{n-1} + p_0 q_0\right) - \lambda_c^{(n)} \geq R \tag{2.10c}$$

$$\sum_{i=0}^{n-1} \lambda_v \left(p_i - p_i q_i\right) < C\left(n\mu_c\right) \tag{2.10d}$$

$$\lambda_v p_0 q_0 < \mu_c \tag{2.10e}$$

$$\sum_{i=0}^{n-1} p_i = 1,\ 0 \leq p_i \leq 1 \qquad i = 0, \ldots, n-1 \tag{2.10f}$$

$$0 \leq q_i \leq 1 \qquad i = 0, \ldots, n-1 \tag{2.10g}$$

$$R > 0 \tag{2.10h}$$

The n constraints in (2.10b) and (2.10c) represent the epigraph form constraints on the original objective function in the right hand side of (2.9), after separation [41] and substituting every $\lambda_v^{(i)}$ by its expansion form in (2.2). The constraints in (2.10d) and (2.10e) represent the stability conditions on charging queues. The constraints in (2.10f) and (2.10g) are the axiomatic constraints on probabilities (i.e., values being between 0 and 1, and sum equal to 1). Finally, Constraint (2.10h) is a strict positivity constraint on the minimum expected response rate, which also guarantees the stability of the customer queues when combined with (2.10b) and (2.10c). Indeed, if R is strictly positive, this guarantees that that the stability conditions in (2.3) hold with certainty. Clearly, the above problem is a linear program with linear constraints, which can be solved analytically using Lagrangian analysis. This will be the target of the next subsection.

2.3.2 Optimal Dispatching and Charging Decisions

The problem in (2.10) is a convex optimization problem with second order differentiable objective and constraint functions that satisfies Slater's condition. Consequently, the KKT conditions provide necessary and sufficient conditions for optimality. Therefore, applying the KKT conditions to the constraints of the problem and the gradient of the Lagrangian function allows us to find the analytical solution of the decisions q_i. The Lagrangian function associated with the optimization problem in (2.10) is given by the following expression:

$$\begin{aligned} L\left(\mathbf{q}, R, \boldsymbol{\alpha}, \boldsymbol{\beta}, \boldsymbol{\gamma}, \boldsymbol{\omega}\right) &= -R + \sum_{i=1}^{n-1} \alpha_i \left(\lambda_v \left(p_{i-1} q_{i-1} - p_i q_i\right) + R - \lambda_v p_{i-1} + \lambda_c^{(i)}\right) \\ &+ \alpha_n \left(\lambda_v \left(p_{n-1} q_{n-1} - p_0 q_0\right) + R - \lambda_v p_{n-1} + \lambda_c^{(n)}\right) + \beta_0 \left(\sum_{i=0}^{n-1} \lambda_v \left(p_i - p_i q_i\right) - C\left(n \mu_c\right)\right) \\ &+ \beta_1 \left(\lambda_v p_0 q_0 - \mu_c\right) + \sum_{i=0}^{n-1} \gamma_i \left(q_i - 1\right) - \sum_{i=0}^{n-1} \omega_i q_i + \omega_n R \end{aligned} \tag{2.11}$$

where $\mathbf{q}$ is the vector of dispatching decisions (i.e. $\mathbf{q} = [q_0, \ldots, q_{n-1}]$), and where:

- $\boldsymbol{\alpha} = [\alpha_i]$, such that α_i is the Lagrange multiplier of the i-th customer queues inequality.
- $\boldsymbol{\beta} = [\beta_i]$, such that βi is the Lagrange multiplier of the i-th charging queues inequality.
- $\boldsymbol{\gamma} = [\gamma_i]$, such that γ_i is the Lagrange multiplier of the i-th upper bound inequality.
- $\boldsymbol{\omega} = [\omega_i]$, such that ω_i is the Lagrange multiplier of the i-th lower bound inequality.

By applying the KKT conditions on the equality and inequality constraints, the following theorem illustrates the optimal solution of the problem in (2.10).

Theorem 1. *The optimal charging/dispatching decisions of the optimization problem in*

(2.10) can be expressed as follows:

$$
\begin{aligned}
q_0^* &= \begin{cases} 0 & \text{if } \alpha_1^* > \alpha_n^* \\ 1 & \text{if } \alpha_1^* < \alpha_n^* \end{cases} \\
q_i^* &= \begin{cases} 0 & \text{if } \alpha_{i+1}^* > \alpha_i^* \\ 1 & \text{if } \alpha_{i+1}^* < \alpha_i^* \end{cases} \qquad i = 1, \ldots, n-1 \\
&\text{if } \alpha_1^* = \alpha_n^* \neq 0 \begin{cases} q_1^* = \frac{p_0 q_0^*}{p_1} - \frac{\lambda_v p_0 - \lambda_c^{(1)} - R^*}{\lambda_v p_1} \\ q_{n-1}^* = \frac{p_0 q_0^*}{p_{n-1}} - \frac{\lambda_v p_0 - \lambda_c^{(n)} - R^*}{\lambda_v p_{n-1}} \end{cases} \\
&\text{if } \alpha_{i+1}^* = \alpha_i^* \neq 0 \begin{cases} q_i^* = \frac{p_{i-1} q_{i-1}^*}{p_i} - \frac{\lambda_v p_{i-1} - \lambda_c^{(i)} - R^*}{\lambda_v p_i} \\ q_{i+1}^* = \frac{p_i q_i^*}{p_{i+1}} - \frac{\lambda_v p_i - \lambda_c^{(i+1)} - R^*}{\lambda_v p_{i+1}} \end{cases} \qquad i = 1, \ldots, n-1
\end{aligned}
\tag{2.12}
$$

Proof. The proof of Theorem 1 is in Appendix C. □

2.3.3 Maximum Expected Response Time

Again, since the problem in (2.10) is convex with differentiable objective and constraint functions, then strong duality holds, which implies that the solution to the primal and dual problems are identical. By solving the dual problem, we can express the optimal value of the maximum expected response time as the reciprocal of the minimum expected response rate of the system. The latter is characterized by the following theorem.

Theorem 2. *The minimum expected response rate R^* of the entire system can be expressed as:*

$$
R^* = \sum_{i=1}^{n} \left(\lambda_v p_{i-1} - \lambda_c^{(i)} \right) \alpha_i^* + \sum_{i=0}^{n-1} \gamma_i^* \tag{2.13}
$$

Proof. The proof of Theorem 2 is in Appendix D. □

2.4 Average Response Time Optimization

The goal of this section is to minimize the average expected response time of the system over all customer classes.

2.4.1 Problem Formulation

As stated earlier, the expected response time for each of the classes in the system is expressed as in (2.7). Since our system is divided to n classes, the average expected response time across the different classes is expressed as:

$$\frac{1}{n}\sum_{i=1}^{n}\frac{1}{\lambda_v^{(i)}-\lambda_c^{(i)}} \tag{2.14}$$

Therefore, minimizing the average expected response time across all the classes of the system, while obeying its stability conditions, can be formulated by the following problem.

$$\underset{q_0,q_1,\ldots,q_{n-1}}{\text{minimize}} \quad \frac{1}{n}\sum_{i=1}^{n}\frac{1}{\lambda_v^{(i)}-\lambda_c^{(i)}} \tag{2.15a}$$

s.t.

$$\lambda_v\left(p_{i-1}-p_{i-1}q_{i-1}+p_iq_i\right)-\lambda_c^{(i)}>0,\ i=1,\ldots,n-1 \tag{2.15b}$$

$$\lambda_v\left(p_{n-1}-p_{n-1}q_{n-1}+p_0q_0\right)-\lambda_c^{(n)}>0 \tag{2.15c}$$

$$\sum_{i=0}^{n-1}\lambda_v\left(p_i-p_iq_i\right)<C\left(n\mu_c\right) \tag{2.15d}$$

$$\lambda_v p_0 q_0<\mu_c \tag{2.15e}$$

$$\sum_{i=0}^{n-1}p_i=1,\ 0\le p_i\le 1 \qquad i=0,\ldots,n-1 \tag{2.15f}$$

$$0\le q_i\le 1 \qquad i=0,\ldots,n-1 \tag{2.15g}$$

The n constraints in (2.15b) and (2.15c) represent the stability constraints in (2.3) and substituting every $\lambda_v^{(i)}$ by its expansion form in (2.2). The constraints in (2.15d) and (2.15e) represent the stability conditions on charging queues. The constraints in (2.15f) and (2.15g) are the axiomatic constraints on probabilities (i.e., values being between 0 and 1, and sum equal to 1).

The above constraints are all linear but the objective function is obviously not. Nonetheless, the following lemma proofs that the optimization problem we have is convex which allows us to find an absolute exact solution analytically and numerically.

Lemma 3. *Defining the function f as follows:*

$$f\left(q_0, q_1, \ldots, q_{n-1}\right) = \frac{1}{n} \sum_{i=1}^{n} \frac{1}{\lambda_v^{(i)} - \lambda_c^{(i)}} \tag{2.16}$$

such that $\lambda_v^{(i)}$ and $\lambda_c^{(i)}$ are defined in (2.2) and (2.3), then the function f is convex over the variables $q_0, q_1, \ldots, q_{n-1}$.

Proof. The proof of Lemma 3 is in Appendix E. □

Consequently, the problem in (2.15) is a convex problem with linear constraints, which can be solved analytically using Lagrangian analysis. This will be the target of the next subsection.

2.4.2 Optimal Dispatching and Charging Decision

As proven above, the problem in (2.15) is a convex optimization problem with second order differentiable objective function and constraints that satisfies Slater's condition. Similar to the approach of Section 2.3.2, we can apply the KKT conditions to the constraints of the problem and the gradient of the Lagrangian function to find the analytical solution of the decisions q_i. The Lagrangian function associated with the optimization problem in (2.15) is

given by the following expression:

$$L\left(\mathbf{q},\boldsymbol{\alpha},\boldsymbol{\beta},\boldsymbol{\gamma},\boldsymbol{\omega}\right)=\frac{1}{n}\sum_{i=1}^{n-1}\frac{1}{\lambda_v\left(p_{i-1}-p_{i-1}q_{i-1}+p_iq_i\right)-\lambda_c^{(i)}}+\beta_0\left(\sum_{i=0}^{n-1}\lambda_v\left(p_i-p_iq_i\right)-C\left(n\mu_c\right)\right)$$
$$+\sum_{i=1}^{n-1}\alpha_i\left(\lambda_c^{(i)}-\lambda_v\left(p_{i-1}-p_{i-1}q_{i-1}+p_iq_i\right)\right)+\alpha_n\left(\lambda_c^{(n)}-\lambda_v\left(p_{n-1}-p_{n-1}q_{n-1}+p_0q_0\right)\right)$$
$$+\beta_1\left(\lambda_vp_0q_0-\mu_c\right)+\sum_{i=0}^{n-1}\gamma_i\left(q_i-1\right)-\sum_{i=0}^{n-1}\omega_iq_i+\frac{1}{n\left(\lambda_v\left(p_{n-1}-p_{n-1}q_{n-1}+p_0q_0\right)-\lambda_c^{(n)}\right)} \tag{2.17}$$

where $\mathbf{q}$ is the vector of dispatching decisions (i.e. $\mathbf{q}=[q_0,\ldots,q_{n-1}]$), and where $\boldsymbol{\alpha}=[\alpha_i]$, $\boldsymbol{\beta}=[\beta_i]$, $\boldsymbol{\gamma}=[\gamma_i]$, $\boldsymbol{\omega}=[\omega_i]$ are the vectors of the Lagrange multipliers associated with the inequalities constraints of the problem (2.15), and defined in the same way explained in Section 2.3.2.

By applying the KKT conditions on the equality and inequality constraints, the following theorem illustrates the optimal solution of the problem in (2.15).

Theorem 3. *The optimal charging/dispatching decisions of the optimization problem in (2.15) can be expressed as follows:*

$$q_i^*=\begin{cases}0 & \text{if } \omega_i^*\neq 0\\ & \\ 1 & \text{if } \gamma_i^*\neq 1\end{cases}\qquad i=0,\ldots,n-1 \tag{2.18}$$

Otherwise, we have:

$$\begin{aligned}q_0^*&=\frac{\lambda_v\left(p_0+p_1q_1^*-p_{n-1}+p_{n-1}q_{n-1}^*\right)-\lambda_c^{(1)}+\lambda_c^{(n)}}{2\lambda_vp_0}\\ q_i^*&=\frac{\lambda_v\left(p_i+p_{i+1}q_{i1}^*-p_{i-1}+p_{i-1}q_{i-1}^*\right)-\lambda_c^{(i+1)}+\lambda_c^{(i)}}{2\lambda_vp_i}\qquad i=1,\ldots,n-2\\ q_{n-1}^*&=\frac{\lambda_v\left(p_{n-1}+p_0q_0^*-p_{n-2}+p_{n-2}q_{n-2}^*\right)-\lambda_c^{(n)}+\lambda_c^{(n-1)}}{2\lambda_vp_{n-1}}\end{aligned} \tag{2.19}$$

Proof. The proof of Theorem 3 is in Appendix F. □

2.5 Simulation Results

In this section, we test the merits of our proposed scheme using extensive simulations. The metrics used to evaluate these merits are the maximum and average expected response times of the different classes. For all the performed simulation figures, the full-charging rate of a vehicle is set to $\mu_c = 0.033$ mins^{-1}, and the number of charging points $C = 40$.

For the optimized maximum and average response time solutions, Figures 2.3a and 2.3b, respectively, illustrate both the interplay of λ_v and $\sum_{i=1}^{n} \lambda_c^{(i)}$, established in Lemma 1, and effect of increasing the number of classes n beyond its strict lower bound introduced in Lemma 2. They depict the maximum and average expected response times for different values of $\sum_{i=1}^{n} \lambda_c^{(i)}$, while fixing λ_v to 15 min^{-1}. For this setting, $n = 12$ is the smallest number of classes that satisfy the stability condition in Lemma 2. It is easy to notice that the response times for all values of n increase dramatically when the $\sum_{i=1}^{n} \lambda_c^{(i)}$ approaches λ_v thus bringing the system closer to its stability limit established in Lemma 1. As also expected, the figures clearly shows that further increasing n beyond its stability lower bound increases both the maximum and average response times. As explained earlier, this effect occurs when due to the reduced number of available vehicles to each customer class as n grows given fixed λ_v. We thus firmly conclude that the optimal number of classes is the smallest value satisfying Lemma 2:

$$n^* = \begin{cases} \dfrac{\lambda_v}{C\mu_c} - \dfrac{1}{C} + 1 & \text{if } \dfrac{\lambda_v}{C\mu_c} - \dfrac{1}{C} \text{ is integer} \\ \left\lceil \dfrac{\lambda_v}{C\mu_c} - \dfrac{1}{C} \right\rceil & \text{Otherwise} \end{cases} \tag{2.20}$$

For the maximum and average response time optimization solutions, Figures 2.4a and 2.4b, respectively, depict the maximum and average expected response time performances for different distributions of the vehicle SoC and customer trip distances, given $\lambda_v = 8$ and thus $n^* = 7$. By decreasing vehicle SoC distribution, we mean that the probability of an arriving

vehicle to have class i SoC is lower than that of it having class $i-1$ SoC $\forall\ i \in \{2,\ldots,n\}$. We can infer from both figures that both the maximum and average response times for Gaussian distributions of trip distances and both Gaussian or decreasing ones for SoCs are the lowest and exhibit the least response time variance. Luckily, these are the most realistic distributions for both variables. This is justified by the fact that vehicles arrive to the system after trips of different distances, which makes their SoC either Gaussian or slightly decreasing. Likewise, customers requiring mid-size distances are usually more than those requiring very small and very long distances.

For the maximum and average response time optimization solutions, Figures 2.5a and 2.5b, respectively, compare the maximum and average expected response times performances against $\sum_{i=1}^{n} \lambda_c^{(i)}$, for different decision approaches, namely our derived optimal decisions in Section 2.3, always partially charge decisions (i.e. $q_i = 0\ \forall\ i$) and equal split decisions (i.e. $q_i = 0.5\ \forall\ i$), for $\lambda_v = 8$ and thus $n = 7$. The latter two schemes represent non-optimized policies, in which each vehicle takes its own fixed decision irrespective of the system parameters. The figures clearly show superior maximum and average performances for our derived optimal policies compared to the other two policies, especially as $\sum_{i=1}^{n} \lambda_c^{(i)}$ gets closer to λ_v, which are the most properly engineered scenarios (as large differences between these two quantities results in very low utilization). Gains of 13.3% and 21.3% in the average and maximum performances, respectively, can be noticed compared to the always charge policy. This demonstrates the importance of our proposed scheme in achieving lower response times and thus better customer satisfaction.

Fig. 2.6 compares the maximum and average expected response time performance given by the maximum and average response time optimization solutions introduced in Sections 2.3 and 2.4, respectively, for different values of the $\sum_{i=1}^{n} \lambda_c^{(i)}$ while fixing λ_v to 15 min^{-1} (i.e., $n^* = 12$). We can easily notice that the maximum expected response times achieved by both solutions are the same. On the other hand, the average expected response time given by the average solution is slightly lower than that of the maximum solution. These

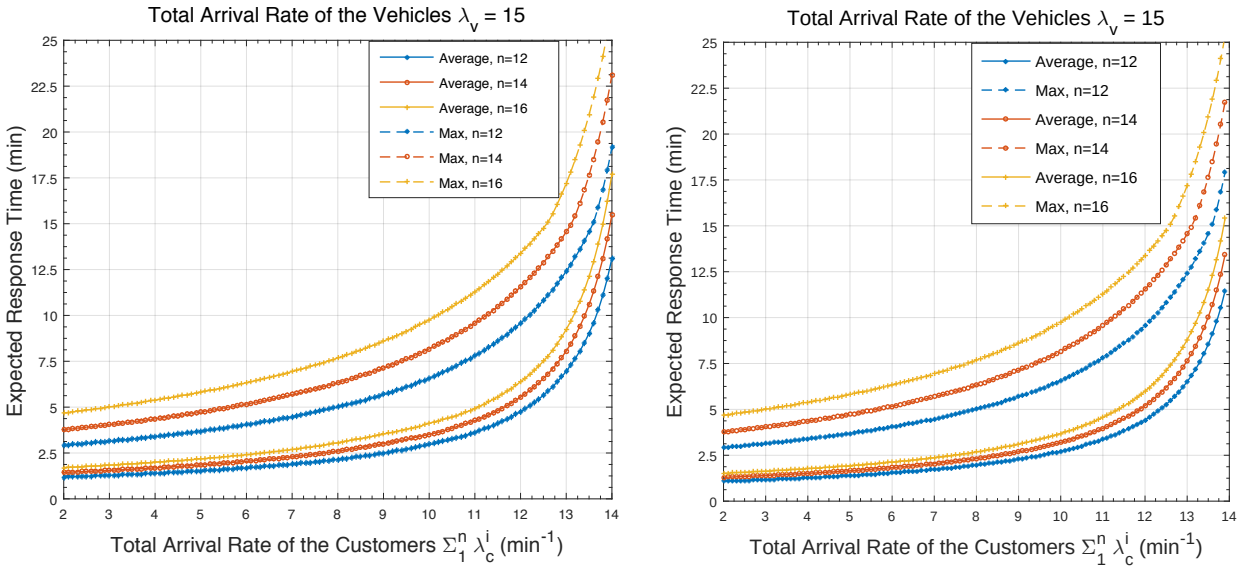

(a) (b)

Figure 2.3: Expected response times using the maximum response time optimization solution for different $\sum_{i=1}^{n} \lambda_c^{(i)}$ and Expected response times using the average response time optimization solution for different $\sum_{i=1}^{n} \lambda_c^{(i)}$

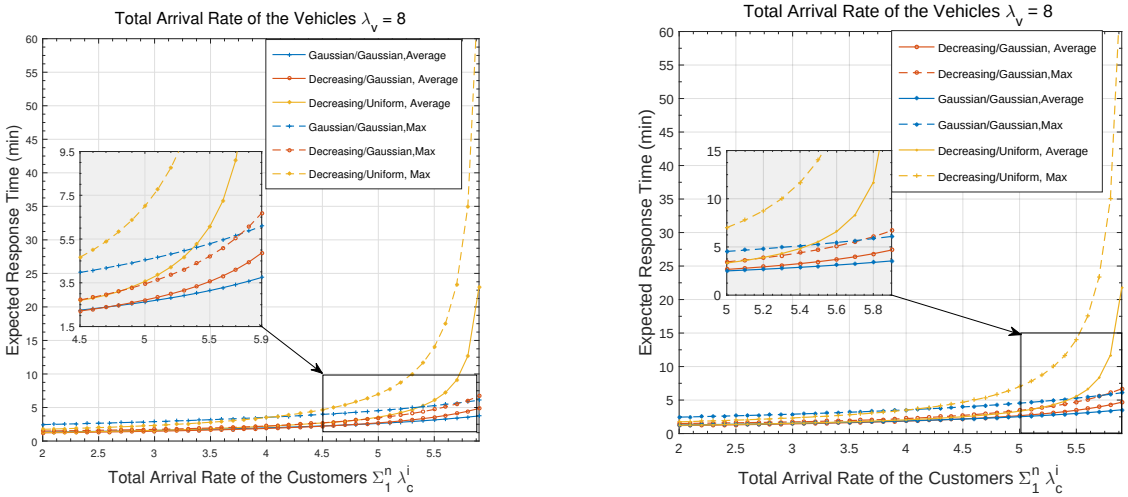

(a) (b)

Figure 2.4: Effect of different customer and SoC distributions on the maximum response time optimization solution and Effect of different customer and SoC distributions on the average response time optimization solution.

results suggest that the variance in performance achieved by both solutions is negligible. Consequently, the one that is obtained using less complexity should be used to almost satisfy the minimum value for both metrics. We know from Sections 2.3 and 2.4 that the maximum

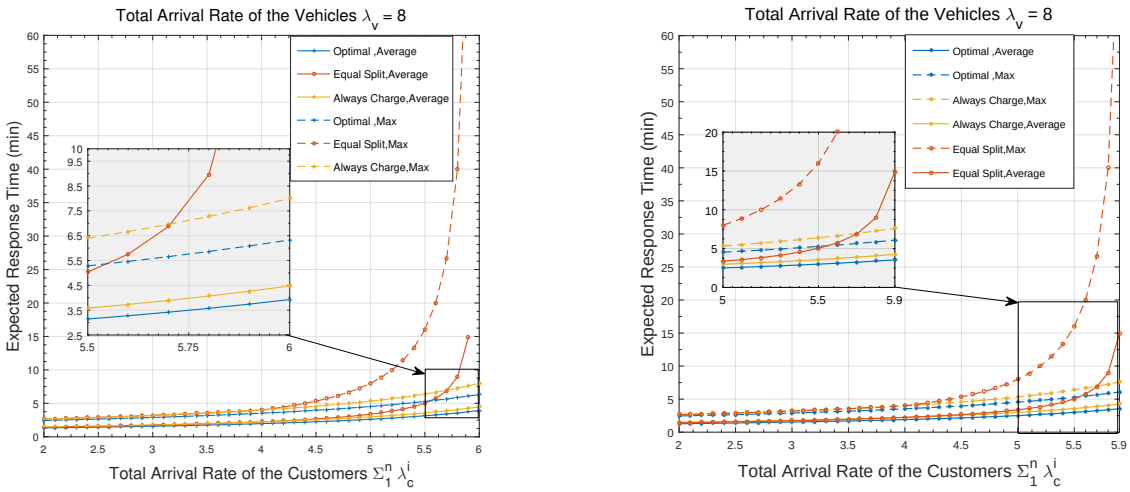

(a) (b)

Figure 2.5: Comparison of the maximum response time optimization solution to non-optimized policies and Comparison of the average response time optimization solution to non-optimized policies.

and average solutions are obtained by solving linear and convex yet non-linear optimizations, respectively. It is well known that solving the latter requires more computations that the former. For example, when using Interior-point methods, the maximum number of iterations for the maximum and average solutions are 10 and 25, respectively. Thus, the use of the maximum solution is recommended in future AEMoD sytems due to its lower complexity and its negligible degradation in its average response time performance compared to the average solution.

Conclusion

In this chapter, we proposed solutions to the computational and charging bottlenecks threatening the success of AEMoD systems by employing a fog-based architecture to distribute the optimization loads over different service zones, reduce communication delays. We also proposed a multi-class dispatching and charging scheme to guarantee the fitness of the vehicle charge requirements for customer trips with the available resources in each city zone. To efficiently engineer this multi-class solution, we developed its queuing model, derived its

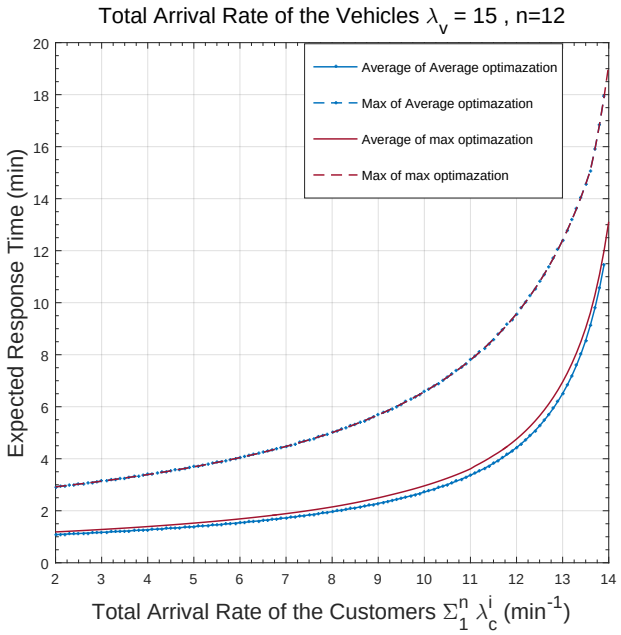

Figure 2.6: Comparison between the maximum minimization and the average minimization of the expected response time

stability conditions, and characterized the optimal number of classes to both minimize the response time and match the zone charging resources. We then formulated the problem of optimizing the proportions of vehicles of each class that will partially/fully charge or directly serve customers as a stochastic linear and convex optimization problems, in order to minimize the maximum and average expected system response times of the system, respectively. The optimal decisions for both problems were analytically derived using Lagrangian analysis. Simulation results demonstrated both the merits of our proposed optimal decision scheme compared to typical non-optimized schemes, and its performance for different distributions of vehicle SoC and customer trip distances. The comparison between the maximum and average problem solutions exhibited negligible variance, which favored the use of the maximum solution due to its lower complexity.

CHAPTER 3

Optimal Vehicle Dimensioning for Multi-Class AMODS

[3] "Optimal Vehicle Dimensioning for Multi-Class Autonomous Electric Mobility On-Demand Systems," *IEEE International Communication Conference (ICC)*, 2018.

Introduction

While the proposed architecture, multi-class, and joint dispatching and charging optimization in the previous chapter seems very promising, the study assumed a constant vehicle in-flow to each zone. Though this typical by the active vehicle in-flow to the system (in-flow of vehicles dropping customers in this zone), the zone demand may require more (less) vehicles at any time of the day, which may call for relocating excess vehicles from (to) neighboring zones. One one hand, serving customers within bounded response times can be guaranteed by injecting more vehicles to each zone. On the other hand, one of the key goals of AEMoD systems is to reduce the congestion. Therefore, determining the optimal number of needed vehicles (dimensioning) to stably serve each zone with bounded response time guarantees is very crucial factor in the operation and key goals of AEMoD systems. In addition, such systems need to be resilient and maintain their stability in special conditions like low charging resources, limited vehicles availability. In this chapter, we work on the system model proposed in the previous chapter. This chapter focuses on finding the optimal vehicle dimensioning for each zone of these systems in order to guarantee a bounded response time of its vehicles. We first derive the stability conditions of the system. Most of the stability conditions are already defined and formulated in the previous chapter. We derive the number of system classes to guarantee the response time bound. Decisions on the proportions of each class vehicles to partially/fully charge, or directly serve customers are then optimized so as to minimize the vehicles in-flow to any given zone. Excess waiting times of customers in rare critical events, such as limited charging resources and/or limited vehicles availabilities, are

also investigated. Results show the merits of our proposed model compared to other schemes and in usual and critical scenarios.

3.1 System Stability and Response Time Limit Conditions

In this section, we first deduce the stability conditions of the proposed system using the basic laws of queuing theory. We will also derive a lower bound on the number of classes n that fits the customer demands, average response time limit, and charging capabilities of any arbitrary service zone. As shown in Fig. 2.2, each of the n customer classes is served by a separate queue of vehicles having a vehicle in-flow rate $\lambda_v^{(i)}$. Consequently, represents . From the aforementioned vehicle dispatching and charging dynamics in Section 2.1, illustrated in Fig. 2.2, the expressions of the service rate of the customer arrival in the i^{th} queue $\lambda_v^{(i)}$ was given in the chapter 2 by the equation 2.2.The stability condition customers queues, was derived in equation 2.3. Moreover, The stability constraints on the C charging points and one central charging station queues were given by the equations 2.4.

It is also established from M/M/1 queue analysis that the average response time for any customer in the i-th class can be expressed as:

$$\frac{1}{\lambda_v^{(i)} - \lambda_c^{(i)}} \tag{3.1}$$

To guarantee customers' satisfaction, the fog controller of each zone must impose an average response time limit T for any class. We can thus express this average response time constraint for the customers of the i-th class as:

$$\frac{1}{\lambda_v^{(i)} - \lambda_c^{(i)}} \leq T \tag{3.2}$$

which can also be re-written as:

$$\lambda_v^{(i)} - \lambda_c^{(i)} \geq \frac{1}{T} \tag{3.3}$$

The following lemma sets a lower bound on the average vehicle in-flow rate to the entire service zone to guarantee both its stability and the average response time limit fulfillment for all its classes, given their demand rates.

Lemma 4. *For the entire zone stability, and fulfillment of the average response time limit for all its classes, the average vehicles in-flow rate must be lower bounded by:*

$$\lambda_v \geq \sum_{i=1}^{n} \lambda_c^{(i)} + \frac{n}{T} \tag{3.4}$$

Proof. The proof of Lemma 4 is in Appendix G. □

Furthermore, the following lemma establishes a lower bound on the number of classes n that fits zone's customer demands, average response time limit, and charging capabilities.

Lemma 5. *For stablize the zone operation given its customer demands, average response time limit, and charging capabilities, the number of classes n in the zone must obey the following inequality:*

$$n \geq \frac{\sum_{i=1}^{n} \lambda_c^{(i)} - \mu_c}{C\mu_c - 1/T} \tag{3.5}$$

Proof. The proof of Lemma 5 is in Appendix H. □

3.2 Optimal Vehicle Dimensioning

3.2.1 Problem Formulation

As previously mentioned, this chapter aims to minimize the average vehicle in-flow rate λ_v to the entire zone, given its charging capacity and customer demand rates, while guaranteeing an average response time limit for each class customers. Given the described system dynamics in Section 2.1 and the derived conditions in Section 3.1, the above problem can be formulated

as a stochastic optimization problem as follows:

$$\underset{q_0,q_1,\ldots,q_{n-1}}{\text{minimize}}\ \lambda_v \tag{3.6a}$$

s.t

$$\lambda_c^{(i)} - \lambda_v(p_{i-1} - p_{i-1}q_{i-1} + p_i q_i) + \frac{1}{T} \leq 0,\ i = 1, \ldots, n-1 \tag{3.6b}$$

$$\lambda_c^{(n)} - \lambda_v(p_{n-1} - p_{n-1}q_{n-1} + p_0 q_0) + \frac{1}{T} \leq 0 \tag{3.6c}$$

$$\sum_{i=0}^{n-1} \lambda_v(p_i - p_i q_i) - C(n\mu_c) < 0 \tag{3.6d}$$

$$\lambda_v p_0 q_0 - \mu_c < 0 \tag{3.6e}$$

$$\sum_{i=0}^{n-1} p_i = 1,\ 0 \leq p_i \leq 1,\ i = 0, \ldots, n-1 \tag{3.6f}$$

$$0 \leq q_i \leq 1,\ i = 0, \ldots, n-1 \tag{3.6g}$$

$$\lambda_v \geq \sum_{i=1}^{n} \lambda_c^{(i)} + \frac{n}{T} \tag{3.6h}$$

The n constraints in (3.6b) and (3.6c) represent the stability and response time limit conditions of the system introduced in (3.3), after substituting every $\lambda_v^{(i)}$ by its expansion form in (2.2). The constraints in (3.6d) and (3.6e) represent the stability conditions for the charging queues. The constraints in (3.6f) and (3.6g) are the axiomatic constraints on probabilities (i.e., values being between 0 and 1, and sum equal to 1). Finally, Constraint (3.6h) is the lower bound on λ_v introduced by Lemma (4).

The above optimization problem is a quadratic non-convex problem with second order differentiable objective and constraint functions. Usually, the solution obtained by using the Lagrangian and KKT analysis for such non-convex problems provides a lower bound on the actual optimal solution. Consequently, we propose to solve the above problem by first finding the solution derived through Lagrangian and KKT analysis, then, if needed, iteratively tightening this solution to the feasibility set of the original problem.

3.2.2 Lower Bound Solution

The Lagrangian function associated with the optimization problem in (3.6) is given by the following expression:

$$\begin{aligned} L(\mathbf{q},\lambda_v,\boldsymbol{\alpha},\boldsymbol{\beta},\boldsymbol{\gamma},\boldsymbol{\omega}) &= \lambda_v + \alpha_n(\lambda_v(p_{n-1}q_{n-1} - p_0q_0 - p_{n-1}) + \lambda_c^{(n)} + \frac{1}{T}) \\ &+ \sum_{i=1}^{n-1}\alpha_i(\lambda_v(p_{i-1}q_{i-1} - p_iq_i - p_{i-1}) + \lambda_c^{(i)} + \frac{1}{T}) + \beta_0(\sum_{i=0}^{n-1}\lambda_v(p_i - p_iq_i) - Cn\mu_c + \epsilon_0) \\ &+ \beta_1(\lambda_v p_0q_0 - \mu_c + \epsilon_1) + \sum_{i=0}^{n-1}\gamma_i(q_i - 1) - \sum_{i=0}^{n-1}\omega_i q_i - \omega_n(\lambda_v - \sum_{i=1}^{n}\lambda_c^{(i)} - \frac{n}{T}) \end{aligned} \tag{3.7}$$

where $\mathbf{q}$ is the vector of dispatching decisions (i.e. $\mathbf{q} = [q_0, \ldots, q_{n-1}]$), and where $\boldsymbol{\alpha} = [\alpha_i]$, $\boldsymbol{\beta} = [\beta_i]$, $\boldsymbol{\gamma} = [\gamma_i]$ and $\boldsymbol{\omega} = [\omega_i]$ are the Lagrange multipliers of the system inequalities as defined in section 2.3.2. For more accurate resolutions, two small positive constants ϵ_0 and ϵ_1 are added to the stability conditions on the charging queues to make them non strict inequalities.

Solving the equations given by the KKT conditions on the problem equality and inequality constraints, the following theorem illustrates the optimal lower bound solutions of the problem in (3.6)

Theorem 4. *The lower bound solution of the optimization problem in (3.6), obtained from*

Lagrangian and KKT analysis can be expressed as follows:

$$\lambda_v^* = \begin{cases} \sum_{i=1}^{n} \lambda_c^{(i)} + \frac{n}{T} & \omega_n^* \neq 0 \\ \sum_{i=1}^{n} \alpha_i^* (\lambda_c^{(i)} + \frac{1}{T}) - \beta_0^* (Cn\mu_c - \epsilon_0) - \beta_1^* (\mu_c - \epsilon_1) & \omega_n^* = 0 \end{cases}$$

$$q_0^* = \begin{cases} 0 & \alpha_1^* - \alpha_n^* - \beta_0^* + \beta_1^* > 0 \\ 1 & \alpha_1^* - \alpha_n^* - \beta_0^* + \beta_1^* < 0 \\ \frac{p_{n-1} q_{n-1}^* - p_{n-1}}{p_0} + \frac{\lambda_c^{(n)} + \frac{1}{T}}{\lambda_v p_0} & \alpha_n^* \neq 0 \\ \frac{\mu_c}{\lambda_v^* p_0} & \beta_1^* \neq 0 \\ \zeta_0(\alpha^*, \beta^*, \gamma^*, \lambda_v^*, q^*) & Otherwise \end{cases} \tag{3.8}$$

$$q_i^* = \begin{cases} 0 & \alpha_{i+1}^* - \alpha_i^* - \beta_0^* > 0 \\ 1 & \alpha_{i+1}^* - \alpha_i^* - \beta_0^* < 0 \\ \frac{p_{i-1} q_{i-1}^* - p_{i-1}}{p_i} + \frac{\lambda_c^{(i)} + \frac{1}{T}}{\lambda_v p_i} & \alpha_i^* \neq 0 \\ \zeta_i(\alpha^*, \beta^*, \gamma^*, \lambda_v^*, q^*) & Otherwise \end{cases} \quad i = 1, \ldots, n-1.$$

where $\zeta_i(\alpha^*, \beta^*, \gamma^*, \lambda_v^*, q^*)$ *is the solution that that maximize* $\inf_{\mathbf{q}} L(\mathbf{q}, \alpha^*, \beta^*, \gamma^*, \lambda_v^*)$

Proof. The proof of Theorem 4 is in Appendix I. □

3.2.3 Solution Tightening

As stated earlier, the closed-form solution derived in the previous section from analyzing the constraints' KKT conditions does not always match with the optimal solution of the original optimization problem, and is sometimes a non-feasible lower bound on our problem. Unfortunately, there is no method to find the exact closed-from solution of non-convex optimization. However, starting from the derived lower bound, we can numerically tighten this solution by toward the feasibility set of the original problem. There are several algorithms to iteratively tighten lower bound solutions, one of which is the *Suggest-and-Improve algo-*

rithm algorithm proposed in [44] to tighten non-convex quadratic problems. We will thus propose to employ this method whenever the KKT conditions based solution is not feasible and tightening is required.

3.3 Simulation Results

In this section, we test both the performance and merits of the proposed dimensioning solution for the considered multi-class AEMoD system. The metric of interest in this study is the optimal vehicle in-flow rate to an arbitrary zone of interest. The performance of the proposed dimensioning solution is tested for two possible SoC distributions for in-flow vehicles, namely the decreasing and Gaussian distributions. The former distribution better models the more probable active-vehicle-dominant in-flow scenarios, as such vehicles typically exhibit higher chances of having lower battery charge. The latter distribution models the rarer relocated-vehicle-dominant in-flow scenarios, as such vehicles typically charge for random amounts of times before relocating to the zone of interest. Customers trip distances are always assumed to follow a Gaussian distribution because customers requiring mid-size distances are usually more than those requiring very small and very long distances. For all the performed simulation studies, the full-charging rate of a vehicle is set to $\mu_c = 0.033$ mins^{-1}. Moreover, for Figures 3.1a, 3.1b, and 3.2a, the number of charging poles C is set to 40.

The first important finding of this study is that the obtained solutions using the closed-form expressions in Theorem 1 (i.e., the one derived by applying the KKT conditions) were always feasible solutions to the original problem in (3.6), for the entire broad range of system parameters employed in our simulations. Thus, the derived closed-form solution is in fact the optimal dimensioning solution for a broad range of system settings, and no tightening is needed.

Fig. 3.1a shows the trade-off relation between the average response time limit, total customer demand rate, and the optimal vehicle in-flow rate, for both vehicle SoC distribu-

tions. This curve can be used by the fog controller to get a rough estimate (without exact demand information per class nor optimization of the dispatching and charging dynamics) on its required in-flow rate (and thus whether it needs extra vehicles or have excess vehicles to relocate) for any given customer demand rate and desired response time limit.

Fig. 3.1b illustrates the effect of increasing the number of classes n beyond its lower bound introduced in Lemma 5 for both variable total customer demand rate (while fixing the average response time limits to 5 mins) and variable average response time limits (while fixing the total customer demand rate to 5 min^{-1}) in the left and right sub figures, respectively. Both decreasing and Gaussian SoC distributions are considered. In both sub-figure, the lower bound on the number of classes vary depending on the values of the average response time and the total customer demand rate (as shown in Lemma 2), with maximum values of 14 and 11 for the employed values in the left and right sub-figures, respectively. The results in both figures clearly show that increasing n beyond its lower bound increases the required vehicle in-flow to the zone. We thus conclude that the optimal number of classes is the smallest integer value satisfying Lemma 5.

Fig. 3.2a compares the performance of our proposed optimal vehicle dimensioning scheme with other non-optimized approaches (in which vehicles follow a fixed dispatching/charging policy irrespective of the system parameters) for different values of total customer demand rate (with $T = 5$) and average response time limit (with $\sum_{i=1}^{n} \lambda_c^{(i)} = 5$). The two non-optimized approaches are the always-charge approach (i.e. $q_i = 0 \ \forall \ i$) and the equal-split approach (i.e. $q_i = 0.5 \ \forall \ i$). The figure clearly shows the superior performance of our derived optimal policy compared to the two non-optimized policies, especially for large total customer demand rates and lower average response time limits. For $\sum_{i=1}^{n} \lambda_c^{(i)} = 10$ min^{-1} in the left subfigure, 36% and 44.4% less vehicle in-flow rates are required compared to always-charge and equal-split policies, respectively, for the more typical decreasing SoC dis-

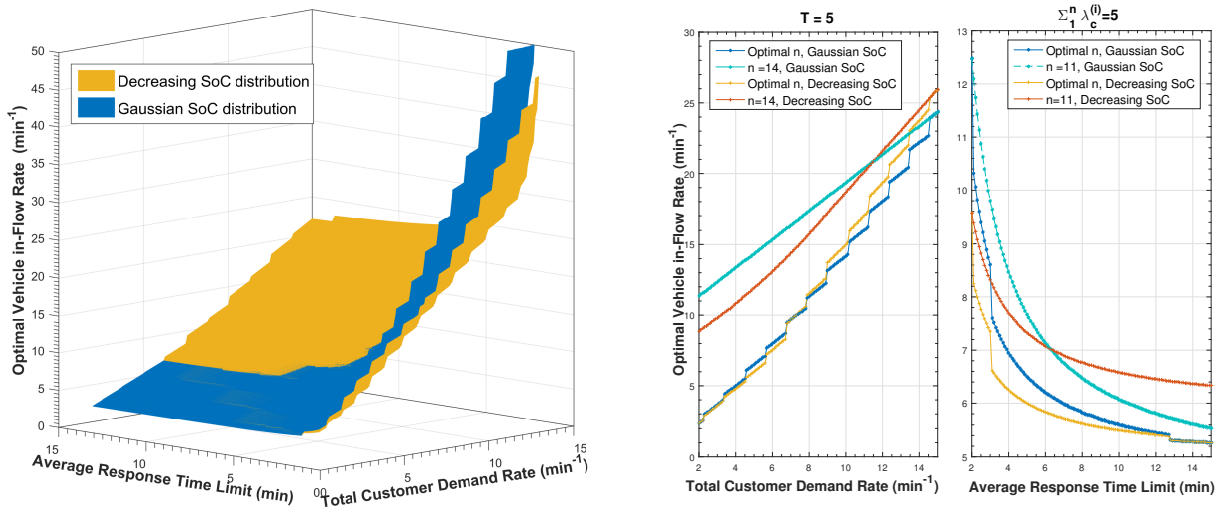

(a) (b)

Figure 3.1: Effect of varying the average response time limit and total customer demand rate and Effect of increasing the number of classes

tribution. These reductions reach 57.6% and 42.5%, respectively for $T = 10$ min in the right subfigure. The always-charge policy is exhibiting less increase in the required vehicle in-flow rate when the SoC follows a Gaussian distribution. However, some considerable gains can still be achieved using our proposed optimized approach in this less frequent SoC distribution setting. Noting that these gains can be higher in more critical scenarios, the results demonstrate the importance of our proposed scheme in establishing a better engineered and more stable system with less vehicles.

Finally, we studied the resilience requirements for our considered model in the critical scenarios of sudden reduction in the number of charging sources within the zone. This reduction may occur due to either natural (e.g., typical failures of one or more stations) or intentional (e.g., a malicious attack on the fog controller blocking its access to these sources). The resilience measures that the fog controller can take in these scenarios is to both notify its customers of a transient increase in the vehicles' response times given the available vehicles in the zone, and request a higher vehicle in-flow rate to gradually restore its original response

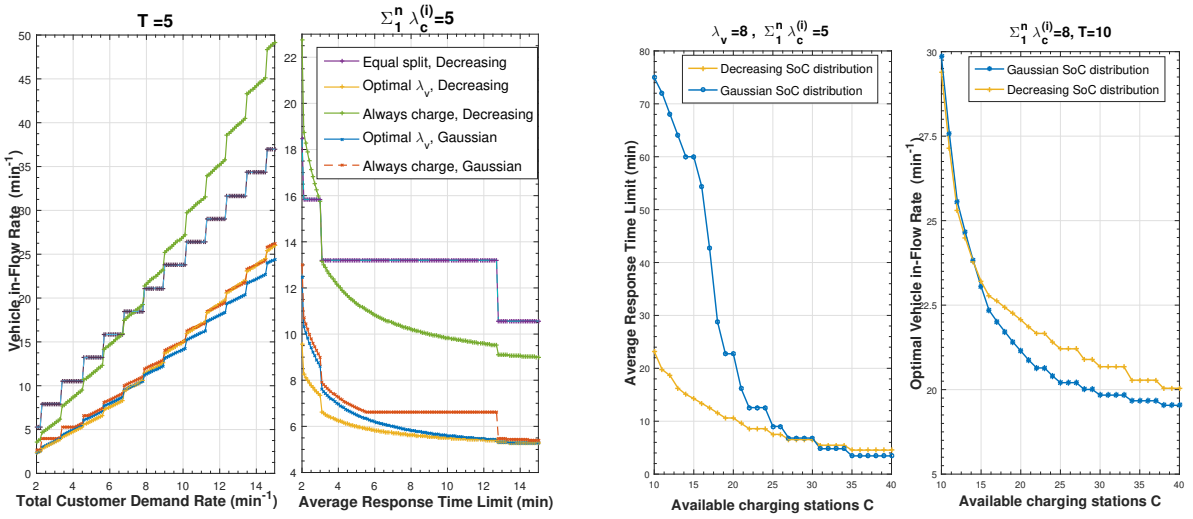

(a) (b)

Figure 3.2: Comparison to non-optimized policies and Effect of varying the charging point availability

time limit.

Our developed optimization framework in [1] and this chapter can easily provide proper numbers for both the above two needed actions by the fog controller in charging station outage events. The problem of computing the maximum transient response time of the system given the fixed vehicle in-flow rate at failure time was already solved in our previous related work [1]. The left subfigure of Fig. 3.2b depicts the maximum response time values of the system for different numbers of available charging poles for a vehicle in-flow rate $\lambda_v = 8$ min^{-1} and a total customer demand rate of 5 min^{-1}. For a Gaussian distribution of vehicles' SoC, the response time increases dramatically when the number of charging poles drops below 20. On the other hand, the degradation in response time was much less severe when the SoC of vehicles follows the decreasing distribution. Luckily, the decreasing SoC distribution is the one that is more probable especially at the time just preceding the failure (where most vehicles arriving to the zone are active vehicles).

As for the recovery from this critical scenario and restoration of the original response time limit, the proposed dimensioning framework in this chapter can be employed to determine

the new optimal value of vehicle in-flow rate. The right sub-figure in Fig. 3.2b depicts the optimal vehicles in-flow λ_v^* for different values of available charging poles C. In this simulation, the total customer demand rate is set to $\sum_{i=1}^{n} \lambda_c^{(i)} = 8$ min^{-1} and the average response time limit is restored back to $T = 10$ mins. The figure shows that the Gaussian SoC distribution case, which would be luckily the dominant case in this zone after failure time (due to the domination of relocated vehicles called in by the fog controller to recover from the failure event), exhibit lower need of vehicle in-flow rate to restore the system conventional operation.

Conclusion

This chapter aimed to formally characterize the optimal vehicle dimensioning for fog-based multi-class AEMoD systems given a system-wide average response time limit. Using the system's queuing model and its stability/response-time constraints, we formulated the optimal vehicle dimensioning problem as a non-convex quadratic program over the multi-class dispatching and charging proportions. The lower bound solution corresponding to the Lagrangian and KKT-conditions analysis of the problem were analytically derived, and were shown to match the optimal solution of the original problem for a broad range of system parameters using extensive simulations. The optimal number of classes to minimize the required vehicle in-flow rate was also characterized. Simulation results demonstrated the merits of our proposed optimal decision scheme compared to other schemes. They also illustrated the resilience requirements calculated using our proposed solutions to recover from sudden reductions in charging resources.

CHAPTER 4

Multi-Class Management with Sub-Class Service for Autonomous Electric Mobility On-Demand Systems

Introduction

Despite the valuable results given by deriving the optimal split proportions for the previously introduced model (compared to typical non-optimized splitting approaches), its dispatching process is not realistic. Indeed, vehicles in this model only sever trips fitting their SoC (before or after partially charging), ignoring the fact that they can also serve all customer classes requesting smaller trips (and thus less charge). This is not only impractical, but can also result in battery depletion of all vehicles by the end of the service, which can cause instabilities to the entire system. In this Chapter, we aim to address this clear limitation of the previous model, by enabling sub-class dispatching; i.e., allowing proportions of each class vehicles to serve to customers from its class as well as all classes requesting shorter trips). The question now is: *What are the optimal charging and sub-classes dispatching proportions to maintain charging stability and minimize the maximum response time of the system?* To address this question, a queuing model representing the proposed multi-class management with sub-class service scheme is first introduced. The stability conditions of this model. Decisions on both the proportions of each class's vehicles to partially/fully charge vs directly dispatch and their proportions of serving own vs sub-classes are then jointly optimized. Finally, the merits of our proposed optimized decision scheme are tested and compared to the proposed work in [1] [3] as well as several non optimized schemes.

4.1 System Model

We consider one service zone controlled by a fog controller connected to: (1) the service request apps of customers in the zone; (2) the AEMoD vehicles; (3) C rapid charging points

distributed in the service zone and designed for short-term partial charging; and (4) one spacious rapid charging station designed for long-term full charging. AEMoD vehicles enter the service in this zone after dropping off their latest customers in it. Their detection as free vehicles by the zone's controller can thus be modeled as a Poisson process with rate λ_v. Customers request service from the system according to a Poisson process. Both customers and vehicles are classified into n classes based on an ascending order of their required trip distance and the corresponding SoC to cover this distance, respectively. From the thinning property of Poisson processes, the arrival process of Class i customers and vehicles, $i \in \{0, \ldots, n\}$, are both independent Poisson processes with rates $\lambda_c^{(i)}$ and $\lambda_v p_i$, where p_i is the probability that the SoC of an arriving vehicle to the system belongs to Class i. Note that p_0 is the probability that a vehicle arrive with a depleted battery, and is thus not able to serve immediately. Consequently, $\lambda_c^{(0)} = 0$ as no customer will request a vehicle that cannot travel any distance. On the other hand, p_n is also equal to 0, because no vehicle can arrive to the system fully charged as it has just finished a prior trip.

Upon arrival, each vehicle of Class i, $i \in \{1, \ldots, n-1\}$, will park anywhere in the zone until it is called by the fog controller to either: (1) join vehicles that will serve customer with their current state of charge with probability q_i (The served customer can be from any Sub-class j with $j \leq i$); or (2) partially charge up to the SoC of class $i+1$ at any of the C charging points (whenever any of them becomes free), with probability $\overline{q}_i = 1 - q_i$, before parking again in waiting to serve a customer from any Sub-class j with $j \leq i+1$. As for Class 0 vehicles that are incapable of serving before charging, they will be directed to either fully charge at the central charging station with probability q_0, or partially charge at one of C charging points with probability $\overline{q}_0 = 1 - q_0$. In the former and latter cases, the vehicle after charging will wait to serve customers of any Sub-class $j \leq n$ and 1, respectively.
Considering the above explanation, Each vehicle, whether decided to serve immediately or decided to charge before serving, will be able to serve: (1) customers from same class with probability Π_{ii}; or (2) customers with a trip distance from any Sub-class with probability

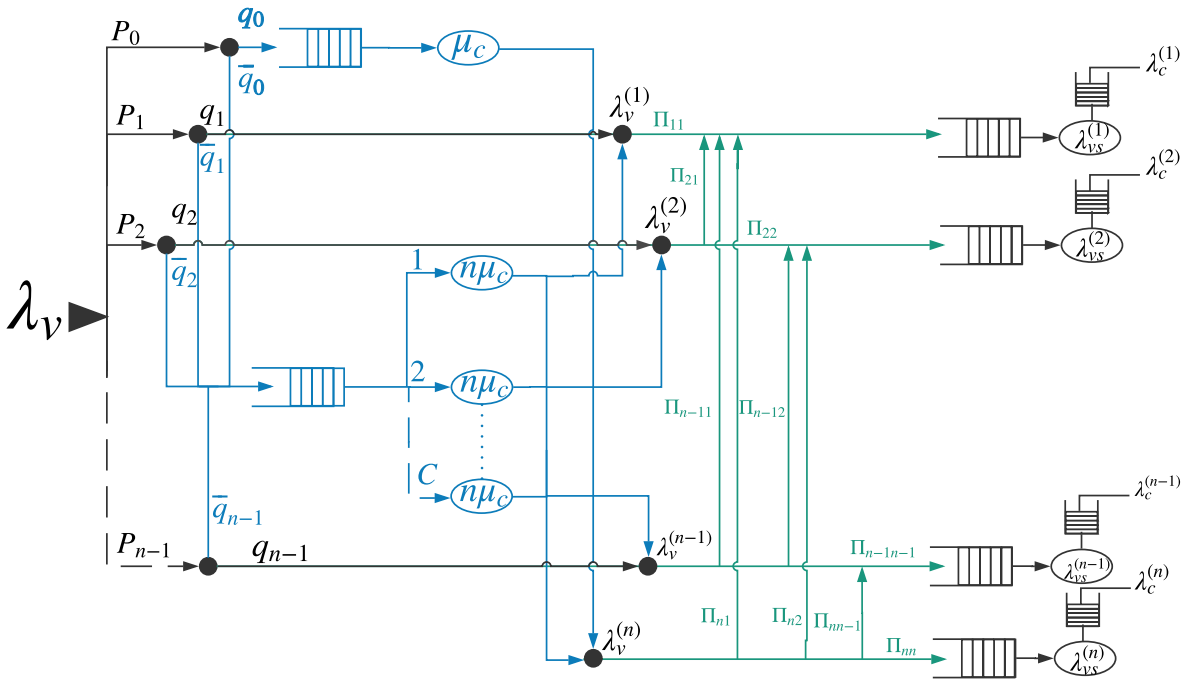

Figure 4.1: Joint dispatching and partially/fully charging model, abstracting an AEMoD system in one service zone.

Π_{ij}.

As widely used in the literature (e.g., [16,17]), the full charging time of a vehicle with a depleted battery is assumed to be exponentially distributed with rate μ_c. Given uniform SoC quantization among the n vehicle classes, the partial charging time can then be modeled as an exponential random variable with rate $n\mu_c$. Note that the larger rate of the partial charging process is not due to a speed-up in the charging process but rather due to the reduced time of partially charging. The customers belonging to Class i, arriving at rate $\lambda_c^{(i)}$, will be served at a rate of $\lambda_{vs}^{(i)}$, which includes summation of proportions of arrival rates of vehicles that: (1) arrived to the zone with a SoC belonging to Class j $\forall j \geq i$ and were directed to wait to serve Class i $\forall i \leq j$ customers; or (2) arrived to the zone with a SoC belonging to Class $j-1$ and were directed to partially charge to be able to serve a Sub-Class i $\forall i \leq j$ customers. Given the above description and modeling of variables, the entire zone dynamics can thus be modeled by the queuing system . This system includes n M/M/1 queues for the n classes of customer service, one M/M/1 queue for the central charging station, and one M/M/C queue

representing the partial charging process at the C charging points.

Our goal in this chapter is to minimize the maximum expected response time of the entire system. By response time, we mean the time needed that vehicle starts moving from its parking or charging spot towards this customer.

4.2 System stability conditions

In this section, we first deduce the stability conditions of our proposed joint dispatching and charging system, using the basic laws of queuing theory. Each class of vehicles with an arrival rate $\lambda_v^{(i)}$ will be characterized by its SoC when it is ready to serve customers. Each of the n classes of customers are served by a separate queue of vehicles, with $\lambda_{vs}^{(i)}$ being the arrival rate of the vehicles that are available to serve the customers of the i^{th} class. Consequently, it is the service rate of the customers i^{th} arrival queues. We can thus deduce from the system model in the previous section the rate of vehicles with SoC that allows to serve a class i or any sub-class $j \leq i$ that requires lower SoC to serve its customers:

$$\begin{aligned} \lambda_v^{(i)} &= \lambda_v(p_{i-1}\overline{q}_{i-1} + p_i q_i),\ i = 1, \ldots, n-1. \\ \lambda_v^{(n)} &= \lambda_v(p_{n-1}\overline{q}_{n-1} + p_0 q_0) \end{aligned} \tag{4.1}$$

Since we know that $\overline{q}_i + q_i = 1$ Then we substitute $\overline{q}_i$ by $1 - q_i$ in order to have a system with n variables

$$\begin{aligned} \lambda_v^{(i)} &= \lambda_v(p_{i-1} - p_{i-1}q_{i-1} + p_i q_i),\ i = 1, \ldots, n-1 \\ \lambda_v^{(n)} &= \lambda_v(p_{n-1} - p_{n-1}q_{n-1} + p_0 q_0) \end{aligned} \tag{4.2}$$

We can also deduce the expression of the rate of vehicles that will actually serve a class of customers i:

$$\lambda_{vs}^{(i)} = \sum_{k=i}^{n} \lambda_v^{(k)} \Pi_{ki},\ i = 1, \ldots, n \tag{4.3}$$

By injecting the expression of λ_v^k in (4.2) in (4.3), we find:

$$\begin{aligned}
\lambda_{vs}^{(i)} &= \lambda_v \sum_{k=i}^{n-1}(p_{k-1} - p_{k-1}q_{k-1} + p_k q_k)\Pi_{ki} + \lambda_v(p_{n-1} - p_{n-1}q_{n-1} + p_0 q_0)\Pi_{ni},\ i = 1, \ldots, n-1 \\
\lambda_{vs}^{(n)} &= \lambda_v(p_{n-1} - p_{n-1}q_{n-1} + p_0 q_0)\Pi_{nn}
\end{aligned} \tag{4.4}$$

From the well-known stability condition of an M/M/1 queue:

$$\lambda_{vs}^{(i)} > \lambda_c^{(i)},\ i = 1, \ldots, n \tag{4.5}$$

To guarantee customers' satisfaction, the fog controller of each zone must impose an average response time limit T for any class. We can thus express this average response time constraint for the customers of the i-th class as:

$$\frac{1}{\lambda_{vs}^{(i)} - \lambda_c^{(i)}} \leq T \text{ or } \lambda_{vs}^{(i)} - \lambda_c^{(i)} \geq R, \text{ with } R = \frac{1}{T} \tag{4.6}$$

Before reaching the customer service queues, the vehicles will go through a decision step of either to go to these queues immediately or partially charge. From the system model, we have the following stability constraints on the C charging points and central charging station queues, respectively:

$$\begin{aligned}
&\sum_{i=0}^{n-1} \lambda_v(p_i - p_i q_i) < C(n\mu_c) \\
&\lambda_v p_0 q_0 < \mu_c
\end{aligned} \tag{4.7}$$

The following lemma allows the estimation of the average needed vehicles arrival for a given service zone.

Lemma 6. *For the entire zone stability, and fulfillment of the average response time limit for all its classes, the average vehicles arrival rate must be lower bounded by:*

$$\lambda_v \geq \sum_{i=1}^{n} \lambda_c^{(i)} + nR \tag{4.8}$$

Proof. The proof of Lemma 6 is in Appendix J □

4.3 Joint Charging and Dispatching optimization

4.3.1 Problem Formulation

The goal of this chapter is to minimize the maximum expected response time of the system's classes. The response time of any class is defined as the average of the duration from any customer request until a vehicle is dispatched to serve him/her. The maximum expected response time is expressed as:

$$\max_{i\in\{1,\dots,n\}} \left\{ \frac{1}{\lambda_{vs}^{(i)} - \lambda_{c}^{(i)}} \right\} \tag{4.9}$$

It is obvious that the system's class having the maximum expected response time is the one that have the minimum expected response rate. In other words, we have:

$$\arg \max_{i\in\{1,\dots,n\}} \left\{ \frac{1}{\lambda_{vs}^{(i)} - \lambda_{c}^{(i)}} \right\} = \arg \min_{i\in\{1,\dots,n\}} \left\{ \lambda_{vs}^{(i)} - \lambda_{c}^{(i)} \right\} \tag{4.10}$$

Consequently, minimizing the maximum expected response time is equivalent to maximizing the minimum expected response rate. Using the epigraph form [41] of the latter problem,

we get the following stochastic optimization problem:

$$\underset{q_0,\ldots,q_{n-1},\Pi_{11},\ldots,\Pi_{nn}}{\text{maximize}} \; R \tag{4.11a}$$

s.t

$$\lambda_v \sum_{k=i}^{n-1}(p_{k-1} - p_{k-1}q_{k-1} + p_k q_k)\Pi_{ki} \tag{4.11b}$$

$$+ \lambda_v(p_{n-1} - p_{n-1}q_{n-1} + p_0 q_0)\Pi_{ni} - \lambda_c^{(i)} \geq R \qquad i = 1, \ldots, n-1 \tag{4.11c}$$

$$\lambda_v(p_{n-1} - p_{n-1}q_{n-1} + p_0 q_0)\Pi_{nn} - \lambda_c^{(n)} \geq R \tag{4.11d}$$

$$\sum_{i=0}^{n-1} \lambda_v(p_i - p_i q_i) < C(n\mu_c) \tag{4.11e}$$

$$\lambda_v p_0 q_0 < \mu_c \tag{4.11f}$$

$$\sum_{j=1}^{i} \Pi_{ij} = 1, \; i = 1, \ldots, n \tag{4.11g}$$

$$0 \leq \Pi_{ij} \leq 1, \; i = 1, \ldots, n, \; j = 1, \ldots, i \tag{4.11h}$$

$$0 \leq q_i \leq 1, \; i = 0, \ldots, n-1 \tag{4.11i}$$

$$\sum_{i=0}^{n-1} p_i = 1, \; 0 \leq p_i \leq 1, \; i = 0, \ldots, n-1 \tag{4.11j}$$

$$0 < R \leq \frac{\lambda_v - \sum_{i=1}^{n} \lambda_c^{(i)}}{n} \tag{4.11k}$$

$$\tag{4.11l}$$

The n constraints in (4.11c) and (4.11d) represent the epigraph form's constraints on the original objective function in the right hand side of (4.10), after separation [41] and substituting every $\lambda_{vs}^{(i)}$ by its expansion form in (4.4). The constraints in (4.11e) and (4.11f) represent the stability conditions on charging queues. The constraints in (4.11g), (4.11h), (4.11i) and (4.11j) are the axiomatic constraints on the probabilities (i.e., values being between 0 and 1, and sum equal to 1). The Finally, Constraint (4.11k) is a positivity constraint on the minimum expected response rate. Finally, Constraint (4.11k) is is a positivity constraint

and the upper bound on R introduced by Lemma (6).

4.3.2 Lower Bound Analytical Solutions

The optimization problem in (4.11) is a quadratic non-convex problem with second order differentiable objective and constraint functions. Usually, the solution obtained by using the Lagrangian and KKT analysis for such non-convex problems provides a lower bound on the actual optimal solution. Consequently, we propose to solve the above problem by first finding the solution derived through Lagrangian and KKT analysis, then, if needed, iteratively tightening this solution to the feasibility set of the original problem. The Lagrangian function associated with the optimization problem in (4.11) is given by the following expression:

$$
\begin{aligned}
L(R, \mathbf{q}, \mathbf{\Pi}, \boldsymbol{\alpha}, \boldsymbol{\beta}, \boldsymbol{\gamma}, \boldsymbol{\omega}, \boldsymbol{\mu}, \boldsymbol{\nu}, \boldsymbol{\delta}) &= -R - \sum_{i=0}^{n-1} \omega_i q_i - \omega_n (R - \epsilon_2) + \sum_{i=1}^{n} \delta_i (\sum_{k=1}^{i} \Pi_{ik} - 1) \\
&+ \sum_{i=1}^{n-1} \alpha_i [\lambda_c^{(i)} - \lambda_v \sum_{k=i}^{n-1} (p_{k-1} - p_{k-1} q_{k-1} + p_k q_k) \Pi_{ki} - \lambda_v (p_{n-1} - p_{n-1} q_{n-1} + p_0 q_0) \Pi_{ni} + R] \\
&+ \alpha_n (\lambda_c^{(n)} - \lambda_v (p_{n-1} - p_{n-1} q_{n-1} + p_0 q_0) \Pi_{ni} + R) + \beta_0 (\sum_{i=0}^{n-1} \lambda_v (p_i - p_i q_i) - C(n \mu_c)) \\
&+ \sum_{i=0}^{n-1} \gamma_i (q_i - 1) + \gamma_n (R - \frac{\lambda_v - \sum_{i=1}^{n} \lambda_c^{(i)}}{n}) + \sum_{i=1}^{n} \sum_{j=1}^{i} \nu_{ij} (\Pi_{ij} - 1) - \mu_{ij} \Pi_{ij} + \beta_1 (\lambda_v p_0 q_0 - \mu_c)
\end{aligned}
\tag{4.12}
$$

where:

- $\mathbf{q} = [q_0, \ldots, q_{n-1}]$ is the vector of charing decisions.
- $\mathbf{\Pi} = [\Pi_{ij}]$ is the vector of dispatching decisions to serve customers.
- $\boldsymbol{\alpha} = [\alpha_i]$, such that α_i is the associated Lagrange multiplier to the i-th customer queues inequality.

- $\boldsymbol{\beta} = [\beta_i]$, such that βi is the associated Lagrange multiplier to the i-th charging queues inequality.

- $\boldsymbol{\delta} = [\delta_i]$, such that δ_i is the associated Lagrange multiplier to the i-th equality constraint on the dispatching decision.

- $\boldsymbol{\gamma} = [\gamma_i]$, such that γ_i is the associated Lagrange multiplier to the i-th upper bound inequality on the charging decisions and the expected response time.

- $\boldsymbol{\omega} = [\omega_i]$, such that ω_i is the associated Lagrange multiplier to the i-th lower bound inequality on the charging decisions and the expected response time.

- $\boldsymbol{\mu} = [\mu_{ij}]$, such that μ_{ij} is the associated Lagrange multiplier to the j-th lower bound inequality on the dispatching decision Π_{ij}.

- $\boldsymbol{\nu} = [\nu_{ij}]$, such that ν_{ij} is the associated Lagrange multiplier to the j-th upper bound inequality on the dispatching decision Π_{ij}.

For more accurate resolutions, Three small positive constants ϵ_0, ϵ_1 and ϵ_2 are added to the stability conditions on the charging queues and the positivity condition on the maximum expected waiting time to make them non strict inequalities.

Solving the equations given by the KKT conditions on the problem equality and inequality constraints, the following theorem illustrates the optimal lower bound solutions of the problem in (4.11).

Theorem 5. *The lower bound solution of the optimization problem in (4.11), obtained from Lagrangian and KKT analysis can be expressed as follows:*

$$
R^* = \begin{cases} \frac{\lambda_v - \sum_{i=1}^{n} \lambda_c^{(i)}}{n} & \gamma_n^* \neq 0 \\ \epsilon_2 & \omega_n^* \neq 0 \\ \sum_{i=1}^{n-1} \alpha_i^* (\lambda_v \sum_{k=i}^{n-1} (p_{k-1} - p_{k-1} q_{k-1}^* + p_k q_k^*) \Pi_{ki}^* + \lambda_v (p_{n-1} - p_{n-1} q_{n-1}^* + p_0 q_0^*) \Pi_{ni}^* - \lambda_c^{(i)}) & \\ + \alpha_n^* (\lambda_v (p_{n-1} - p_{n-1} q_{n-1}^* + p_0 q_0^*) \Pi_{nn}^* - \lambda_c^{(n)}) & Otherwise \end{cases}
$$

$$
q_0^* = \begin{cases} 0 & \alpha_1^* \Pi_{11}^* - \sum_{i=1}^{n} \alpha_i^* \Pi_{ni}^* - \beta_0^* + \beta_1^* > 0 \\ 1 & \alpha_1^* \Pi_{11}^* - \sum_{i=1}^{n} \alpha_i^* \Pi_{ni}^* - \beta_0^* + \beta_1^* < 0 \\ \frac{\lambda_c^{(n)} + \lambda_v p_{n-1} q_{n-1}^* \Pi_{nn}^* - \lambda_v p_{n-1} \Pi_{nn}^* + R^*}{\lambda_v p_0 \Pi n n^*} & \alpha_n^* \neq 0 \\ \frac{\mu_c}{\lambda_v^* p_0} & \beta_1^* \neq 0 \\ \zeta_0(R^*, q^*, \Pi^*, \alpha^*, \beta^*, \gamma^*, \omega^*, \mu^*, \nu^*, \delta^*) & Otherwise \end{cases}
$$

$$
q_i^* = \begin{cases} 0 & \alpha_{i+1}^* - \alpha_i^* - \beta_0^* > 0 \\ 1 & \alpha_{i+1}^* - \alpha_i^* - \beta_0^* < 0 \qquad i = 1, \ldots, n-1. \\ \frac{R^* + \lambda_c^{(i)} + \lambda_v \left[\sum_{k=i+2}^{n-1} (p_{k-1} q_{k-1}^* - p_k q_k^*) \Pi_{ki} + (p_{n-1} q_{n-1}^* - p_0 q_0^*) \Pi_{ni} - \sum_{k=i}^{n} p_{k-1} \Pi_{ki} + p_{i-1} q_{i-1}^* \Pi_{ii}^* - p_{i+1} q_{i+1} \Pi_{i+1 i+1} \right]}{\lambda_v p_i (\Pi_{ii} - \Pi_{i+1 i+1})} & \alpha_i^* \neq 0 \\ \zeta_i(R^*, q^*, \Pi^*, \alpha^*, \beta^*, \gamma^*, \omega^*, \mu^*, \nu^*, \delta^*) & Otherwise \end{cases}
$$

$$
\Pi_{ij}^* = \begin{cases} 0 & \alpha_j^* \lambda_v (p_{i-1} q_{i-1^*} - p_{i-1} - p_i q_i^*) + \delta_i^* > 0 \\ 1 & \alpha_j^* \lambda_v (p_{i-1} q_{i-1^*} - p_{i-1} - p_i q_i^*) + \delta_i^* < 0 \quad i = 1, \ldots, n-1. \\ \zeta_{ij}(R^*, q^*, \Pi^*, \alpha^*, \beta^*, \gamma^*, \omega^*, \mu^*, \nu^*, \delta^*) & Otherwise \end{cases} \tag{4.13}
$$

where ζ_i *and* ζ_{ij} *are the solution that that maximize* $\inf_{\mathbf{q}, \mathbf{\Pi}} L(\mathbf{q}, \Pi^*, R^*, \alpha^*, \beta^*, \gamma^*, \omega^*, \mu^*, \nu^*, \delta^*)$

Proof. The proof of Theorem 5 is in Appendix K. □

4.3.3 Solution Tightening

As stated earlier, the closed-form solution derived in the previous section from analyzing the constraints' KKT conditions does not always match with the optimal solution of the

original optimization problem, and is sometimes a non-feasible lower bound on our problem. Unfortunately, there is no method to find the exact closed-from solution of non-convex optimization. However, starting from the derived lower bound, we can numerically tighten this solution by iterating toward the feasible set of the original problem. There are several algorithms to iteratively tighten lower bound solutions, one of which is the *Suggest-and-Improve algorithm* algorithm proposed in [44] to tighten non-convex quadratic problems. We will thus propose to employ this method whenever the KKT conditions based solution is not feasible and tightening is required.

4.4 Simulation Results

In this section, we test the merits of our proposed scheme using extensive simulations. The metric used to evaluate these merits is the maximum expected response times of the different classes. For all the performed simulation figures, the full-charging rate of a vehicle is set to $\mu_c = 0.033$ mins^{-1}, and the number of charging points $C = 40$.

Fig. 4.2a depicts the maximum expected response time for different values of $\sum_{i=1}^{n} \lambda_c^{(i)}$, while fixing λ_v to 8 min^{-1}. For this setting, $n = 7$ is the smallest number of classes that satisfy the stability condition in Lemma 2 in [1]. From queuing theory rules [42] [43] the more serving queues a system have, the higher the waiting time will be. Moreover, in previous related work [1] [3], we showed that increasing the number of classes n beyond its strict lower bound introduced in Lemma 2 in [1] will damage the system performance and increase the maximum response time.

Fig. 4.2a compare the maximum expected response time performances against $\sum_{i=1}^{n} \lambda_c^{(i)}$, for different decision approaches namely our derived optimal decisions to the following decisions sets:

1. Optimized charging decisions (i.e. $q_i \; \forall \; i$) with same class dispatching (i.e. $\Pi_{ii} = 1 \; \forall \; i$ and $\Pi_{ij} = 0 \; \forall \; i, j \neq i$)

2. Always partially charge decisions (i.e. $q_i = 0 \ \forall \ i$) with same class dispatching (i.e. $\Pi_{ii} = 1 \ \forall \ i$ and $\Pi_{ij} = 0 \ \forall \ i, j \neq i$)

3. Equal split charging decisions (i.e. $q_i = 0.5 \ \forall \ i$) with same class dispatching (i.e. $\Pi_{ii} = 1 \ \forall \ i$ and $\Pi_{ij} = 0 \ \forall \ i, j \neq i$)

4. Always partially charge decisions (i.e. $q_i = 0 \ \forall \ i$) with proportional sub-classes dispatching decisions (i.e. Π_{ij} proportional to the customers sub-classes needs)

5. Equal split charge decisions (i.e. $q_i = 0 \ \forall \ i$) with proportional sub-classes dispatching decisions (i.e. Π_{ij} proportional to the customers sub-classes needs)

These five schemes represent the possible non-optimized policies, in which each vehicle takes its own fixed decision irrespective of the system parameters. These schemes are possible in case of a non connected and optimized system.

Fig. 4.2a compares these approaches with a decreasing SoC distribution. The figure clearly show superior performances for our derived optimal policy compared to the other policies, especially as $\sum_{i=1}^{n} \lambda_c^{(i)}$ gets closer to λ_v, which are the most properly engineers scenarios (as large differences between these two quantities results in very low utilization), This approves the expression found in lemma 6. A Gains of 49.3%, 69.8%, 93.22%, 86.7% and 94.4% in the performances, can be noticed compared to the previously stated policies respectively.

Fig. 4.2b shows the study of the resilience requirements for our considered model in the critical scenarios of sudden reduction in the number of charging sources within the zone. This reduction may occur due to either natural (e.g., typical failures of one or more stations) or intentional (e.g., a malicious attack on the fog controller blocking its access to these sources). The resilience measure that the fog controller can take in these scenarios is to notify its customers of a transient increase in the vehicles' response times given the available vehicles in the zone. For this, we are only comparing the new proposed model to our previously proposed model. The figures shows clearly the advantage brought by

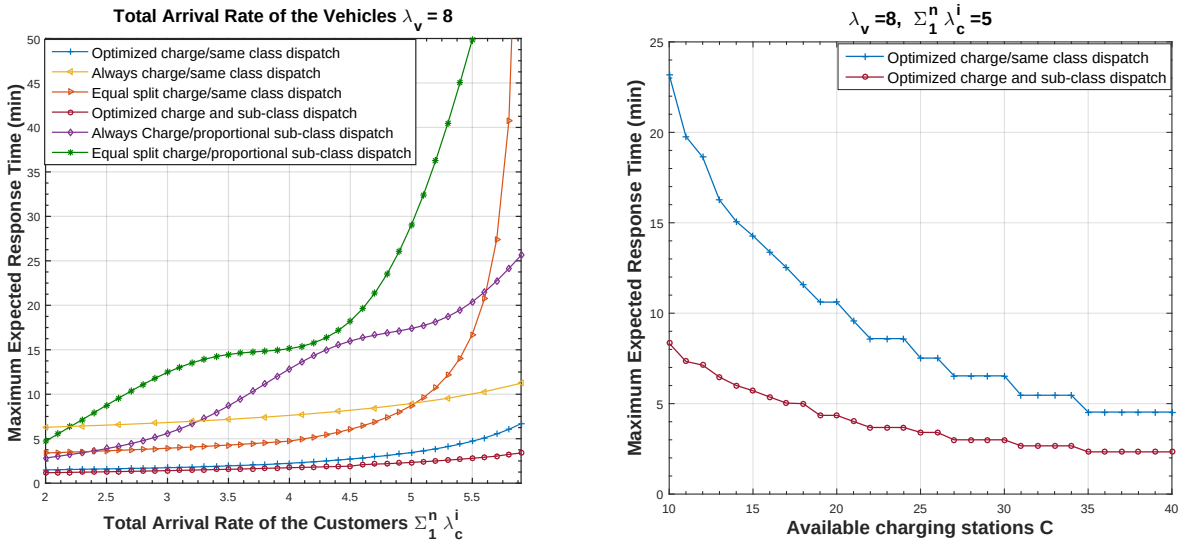

(a) (b)

Figure 4.2: Comparison to non-optimized policies for Decreasing SoC distribution and Effect of varying charging points availability

the sub-class dispatching model. The gain gets higher in critical scenarios and reaches up to 65% with very acceptable maximum response time even is very low energy resources. This demonstrates the importance of our proposed scheme in achieving better customer satisfaction.

Conclusion

In this chapter we proposed a multi-class dispatching and charging scheme and developed its queuing model and stability conditions. We then formulated the problem of optimizing the proportions of vehicles of each class that will partially/fully charge or directly serve customers of same class or any lower sub-class as an optimization problem, in order to minimize the maximum expected system response time while respecting the system stability constraints. The optimal decisions and corresponding maximum response time were analytically derived. Simulation results demonstrated both the merits of our proposed optimal decision scheme compared to typical non-optimized schemes and previously optimized scheme, and its performance for different distributions of vehicle SoC and customer trip distances.

CHAPTER 5

Conclusion

5.1 Summary

In this Thesis, we proposed solutions to the computational and charging bottlenecks threatening the success of AEMoD systems in attracting a large number of customers and solving private urban transportation problems. The computational bottleneck can be resolved by employing a fog-based architecture to distribute the optimization loads over different service zones, reduce communication delays, while which matching the nature of dispatching/charging processes of AEMoD vehicles. We also proposed a multi-class dispatching and charging scheme to guarantee the fitness of the vehicle charge requirements for customer trips with the available resources in each city zone. To efficiently engineer this multi-class solution, we developed its queuing model, derived its stability conditions, and characterized the optimal number of classes to both minimize the response time and match the zone charging resources. We then formulated the problem of optimizing the proportions of vehicles of each class that will partially/fully charge or directly serve customers as a stochastic linear and convex optimization problems, in order to minimize the maximum and average expected system response times of the system, respectively. The optimal decisions for both problems were analytically derived using Lagrangian analysis. Simulation results demonstrated both the merits of our proposed optimal decision scheme compared to typical non-optimized schemes, and its performance for different distributions of vehicle SoC and customer trip distances. The comparison between the maximum and average problem solutions exhibited negligible variance, which favored the use of the maximum solution due to its lower complexity.

The third chapter aimed to formally characterize the optimal vehicle dimensioning for fog-based multi-class AEMoD systems given a system-wide average response time limit. Using the system's queuing model and its stability/response-time constraints, we formulated the optimal vehicle dimensioning problem as a non-convex quadratic program over the multi-

class dispatching and charging proportions. The lower bound solution corresponding to the Lagrangian and KKT-conditions analysis of the problem were analytically derived, and were shown to match the optimal solution of the original problem for a broad range of system parameters using extensive simulations. The optimal number of classes to minimize the required vehicle in-flow rate was also characterized. Simulation results demonstrated the merits of our proposed optimal decision scheme compared to other schemes. They also illustrated the resilience requirements calculated using our proposed solutions to recover from sudden reductions in charging resources.

In the fourth chapter,proposed an enhance multi-class dispatching and charging scheme and developed its queuing model and stability conditions. We then formulated the problem of optimizing the proportions of vehicles of each class that will partially/fully charge or directly serve customers of same class or any lower sub-class as an optimization problem, in order to minimize the maximum expected system response time while respecting the system stability constraints. The optimal decisions and corresponding maximum response time were analytically derived. Simulation results demonstrated both the merits of our proposed optimal decision scheme compared to typical non-optimized schemes and previously optimized scheme, and its performance for different distributions of vehicle SoC and customer trip distances.

5.2 Future Directions

For the future work, we will study the problem of maximizing the system utilization (i.e., minimizing the required in-flow vehicle rate to each city zone) while satisfying a maximum response time constraint for the new proposed model in the chapter four. We will also study scenarios where the charging process of the vehicles is more sophisticated. Most importantly we will study the inter-fog communication and rebalancing processes.

References

[1] S. Belakaria, M. Ammous, S. Sorour, and A. Abdel-Rahim, "A Multi-Class Dispatching and Charging Scheme for Autonomous Electric Mobility On-Demand," *in Proc. of IEEE Vehicular Technology Conference (VTC'17-Fall)*, Toronto, ON, Canada, September 2017.

[2] M. Ammous, S. Belakaria, S. Sorour, and A. Abdel-Rahim, "Optimal Routing with In-Route Charging of Mobility-on-Demand Electric Vehicles",*IEEE Vehicular Technology Conference (VTC2017-Fall)*, Toronto, Canada, 2017.

[3] S. Belakaria, M. Ammous, S. Sorour, and A. Abdel-Rahim, "Optimal Vehicle Dimensioning for Multi-Class Autonomous Electric Mobility On-Demand Systems, " *IEEE International Communication Conference (ICC)*, 2018.

[4] U. E. I. Administration, "International Energy Outlook 2013, " Tech. Rep., 2013.

[5] W. J. Mitchell, C. E. Borroni-Bird, and L. D. Burns, "Reinventing the Automobile: Personal Urban Mobility for the 21st Century". Cambridge, MA: The MIT Press, 2010.

[6] D. Schrank, B. Eisele, and T. Lomax, "TTIs 2012 Urban Mobility Report, " *Texas A&M Transportation Institute*, Texas, USA.2012.

[7] U. N. E. Programme, "The Emissions Gap Report 2013 - UNEP, " *Tech. Rep.*, 2013.

[8] U. E. P. Agency, "Greenhouse Gas Equivalencies Calculator, " *Tech.Rep.*, 2014. [Online]: http://www.epa.gov/cleanenergy/energy-resources/refs.html

[9] A. Santos, N. McGuckin, H. Y. Nakamoto, D. Gray, and S. Liss, "Summary of Travel Trends: 2009 National Household Travel Survey, " *Tech. Rep.*, 2011.

[10] "IoT And Smart Cars: Changing The World For The Better, " *Digitalist Magazine*, August 30, 2016. [Online]: http://www.digitalistmag.com/iot/2016/08/30/iot-smart-connected-cars-willchange-world-04422640

[11] "Transportation Outlook: 2025 to 2050, " *Navigant Research, Q2'16*, 2016. [Online]: http://www.navigantresearch.com/research/transportation-outlook-2025-to-2050.

[12] "The Future Is Now: Smart Cars And IoT In Cities, " *Forbes*, June 13, 2016. [Online]: http://www.forbes.com/sites/pikeresearch/2016/06/13/the-future-is-now-smartcars/63c0a25248c9

[13] "Fog Computing and the Internet of Things: Extend the Cloud to Where the Things Are, " *Cisco White Paper*, 2015. [Online]:http://www.cisco.com/c/dam/en_us/solutions/trends/iot/docs/computing-overview.pdf

[14] R. Zhang, K. Spieser, E. Frazzoli, and M. Pavone, "Models, Algorithms, and Evaluation for Autonomous Mobility-On-Demand Systems, " *in Proc. of American Control Conference*, Chicago, Illinois, 2015.

[15] R. Zhang, F. Rossi, and M. Pavone, "Model Predictive Control of Autonomous Mobility-on-Demand Systems, " *in Proc. IEEE Conference on Robotics and Automation*, Stockholm, Sweden, 2016.

[16] H. Liang, I. Sharma, W. Zhuang, and K. Bhattacharya, "Plug-in Electric Vehicle Charging Demand Estimation based on Queuing Network Analysis, " *IEEE Power and Energy Society General Meeting*, 2014.

[17] K. Zhang, Y. Mao, S. Leng, Y. Zhang, S. Gjessing, and D.H.K. Tsang, "Platoon-based Electric Vehicles Charging with Renewable Energy Supply: A Queuing Analytical Model, " *in Proc. of IEEE International Conference on Communications (ICC'16)*, 2016.

[18] R. Zhang and M. Pacone, "Control of robotic mobility-on-demand systems: a Queuing-Theoretical Perspective, " *ACM International Journal of Robotics Research*, 2016.

[19] K. Treleaven, M. Pavone, and E. Frazzoli, "Asymptotically Optimal Algorithms for One-to-One Pickup and Delivery Problems With Applications to Transportation Systems, " *IEEE Transaction on Automatic Control*, September 2013.

[20] C. Korkas, S. Baldi, S. Yuan, and E.B. Kosmatopoulos, "An Adaptive Learning-based Approach for Nearly-Optimal Dynamic Charging of Electric Vehicle Fleets," *IEEE Transactions on Intelligent Transportation Systems*, 2018.

[21] W. Tang and Y. J. Zhang, "A model predictive control approach for low-complexity electric vehicle charging scheduling: Optimality and scalability," *IEEE Transactions on Power Systems*, 2017.

[22] W. Tushar, C. Yuen, S. Huang, D. B. Smith, and H. V. Poor, "Cost minimization of charging stations with photovoltaics: An approach with ev classification," *IEEE Transactions on Intelligent Transportation Systems*, 2016.

[23] E. S. Rigas, S. D. Ramchurn, and N. Bassiliades, "Managing electric vehicles in the smart grid using artificial intelligence: A survey," *IEEE Transactions on Intelligent Transportation Systems, 16(4):1619-1635*, 2015.

[24] L. Rao and J. Yao, "SmartCar: Smart charging and driving control for electric vehicles in the smart grid," *Proc. IEEE Global Commun. Conf., Dec,* 2014.

[25] S. Bansal, M. N. Zeilinger, and C. J. Tomlin, "Plug-and-play model predictive control for electric vehicle charging and voltage control in smart grids," *Proc. IEEE 53rd Conf. Decision Control,* 2014.

[26] M. Kumru, E. Debada, E. Frazzoli, L. Makarem and D. Gillet "Mobility-on-demand scenarios relying on lightweight autonomous and connected vehicles for large pedestrian areas and intermodal hubs," *in Proc. of Intelligent Transportation Engineering (ICITE)*,Singapore, Singapore, 2017.

[27] S. Kim, G. Gwon, W. Hur, D. Hyeon, D. Kim, S. Kim, D. Kye, S. Lee, S. Lee, M. Shin and S. Seo "Autonomous Campus Mobility Services Using Driverless Taxi," *IEEE Transactions on Intelligent Transportation Systems*,2017

[28] J. Miller, J. How "Predictive positioning and quality of service ride-sharing for campus mobility on demand systems," *Robotics and Automation (ICRA)*,Singapore, Singapore,2017

[29] Y. Mao, C. You, J. Zhang, K. Huang, and K. B. Letaief, "A Survey on Mobile Edge Computing: The Communication Perspective," *IEEE communication surveys & tutorials, VOL. 19, NO. 4, FOURTH QUARTER,* 2017.

[30] "Mobile-edge computing-Introductory technical white paper," White Paper, ETSI, Sophia Antipolis, France, Sep. 2014.

[31] M. Chiang and T. Zhang, "Fog and IoT: An overview of research opportunities," *IEEE Internet Things J., vol. 3, no. 6, pp. 854-864, Dec.* 2016.

[32] G. P. Fettweis, "The tactile Internet: Applications and challenges," *IEEE Veh. Technol. Mag., vol. 9, no. 1, pp. 64-70*, Mar. 2014.

[33] M. Satyanarayanan, P. Bahl, R. Caceres, and N. Davies, "The case for VM-based cloudlets in mobile computing," *IEEE Pervasive Comput., vol. 8, no. 4, pp. 14-23*, Oct./Dec. 2009

[34] T. X. Tran, A. Hajisami, P. Pandey, and D. Pompili, "Collaborative mobile edge computing in 5G networks: New paradigms, scenarios, and challenges," *IEEE Commun. Mag., vol. 55, no. 4, pp. 54-61,* Apr. 2017.

[35] "5G automotive vision," White Paper, 5GPPP, Oct. 2015. [Online]. Available: https://5g-ppp.eu/wp-content/uploads/2014/02/ 5G-PPP-White-Paper-on-Automotive-Vertical-Sectors.pdf

[36] P. Mach, and Z. Becvar, "Mobile Edge Computing: A Survey on Architecture and Computation Offloading", *IEEE communication surveys & tutorials, VOL. 19, NO. 3, THIRD QUARTER,* 2017.

[37] X. Huang, R. Yu, J. Kang, Y. He, and Y. Zhang, "Exploring Mobile Edge Computing for 5G-Enabled Software Defined Vehicular Networks," *IEEE Wireless Communications*, 2017.

[38] A. Somov and R. Giaffreda, "Powering IoT devices: Technologies and opportunities," IEEE IoT Newslett., Nov. 2015. [Online]. Available: http://iot.ieee.org/newsletter/november-2015/powering- iot-devices-technologies-and-opportunities.html

[39] E. K. Markakis, K. Karras, A. Sideris, G. Alexiou, and E. Pallis, "Computing, Caching, and Communication at the Edge: The Cornerstone for Building a Versatile 5G Ecosystem", *IEEE Communications Magazine,* 2017.

[40] E. K. Markakis, I. Politis, A. Lykourgiotis, Y. Rebahi, G. Mastorakis, C. X. Mavromoustakis, and E. Pallis, "Efficient Next Generation Emergency Communications over Multi-Access Edge Computing", *IEEE Communications Magazine,* 2017.

[41] S. Boyd and L. Vandenberghe, "Convex Optimization", 1st ed. *Cambridge: Cambridge University Press*, 2015.

[42] A. Papoulis and S. Pillai, Probability, Random Variables, and Stochastic Processes, 4th ed. International Edition: McGraw-Hill, 2002.

[43] A.L. Garcia, Probability, Statistics, and Random Processes for Electrical Engineering, 3rd ed., Prentice Hall, 2008.

[44] S. Boyd and J. Park, "General Heuristics for Nonconvex Quadratically Constrained Quadratic Programming'. *Stanford University*, 2017.

Appendix A: Proof of Lemma 1

From (2.2) and (2.3) we have:

$$\begin{aligned} \lambda_c^{(i)} &< \lambda_v \left(p_{i-1}\overline{q}_{i-1} + p_i q_i\right) && i = 1, \ldots, n-1 \\ \lambda_c^{(n)} &< \lambda_v \left(p_{n-1}\overline{q}_{n-1} + p_0 q_0\right) && i = n \end{aligned} \tag{5.1}$$

The summation of all the inequalities in (5.1) gives a new inequality

$$\sum_{i=1}^{n} \lambda_c^{(i)} < \lambda_v \left[\sum_{i=1}^{n-1} \left(p_{i-1}\overline{q}_{i-1} + p_i q_i\right) + \left(p_{n-1}\overline{q}_{n-1} + p_0 q_0\right)\right] \tag{5.2}$$

$$\sum_{i=1}^{n} \lambda_c^{(i)} < \lambda_v \left[p_0\overline{q}_0 + p_1 q_1 + p_1\overline{q}_1 + ... + p_{n-1}\overline{q}_{n-1} + p_0 q_0\right] \tag{5.3}$$

We have $\overline{q}_i + q_i$ so $p_i\overline{q}_i + p_i q_i = p_i$

$$\sum_{i=1}^{n} \lambda_c^{(i)} < \lambda_v \left(p_0 + p_1 + p_2 + ... + p_{n-1}\right) \tag{5.4}$$

We have $\sum_{i=0}^{n-1} p_i = 1$ so $\sum_{i=1}^{n} \lambda_c^{(i)} < \lambda_v$

Appendix B: Proof of Lemma 2

The summation of the inequalities given by (2.4)

$\forall\ i = \{0, \ldots, n\}$ gives the following inequality:

$$\lambda_v \sum_{i=0}^{n-1} p_i - \lambda_v \sum_{i=0}^{n-1} p_i q_i + \lambda_v p_0 q_0 < C\left(n\mu_c\right) + \mu_c \tag{5.5}$$

Since $\sum_{i=0}^{n-1} p_i = 1$ (because $p_n = 0$ as described in Section 2), we get:

$$\lambda_v - \lambda_v \sum_{i=1}^{n-1} p_i q_i < \mu_c \left(Cn + 1\right) \tag{5.6}$$

In the worst case, all the vehicles will be directed to partially charge before serving, which means that always $q_i = 0$. Therefore, we get:

$$Cn > \frac{\lambda_v}{\mu_c} - 1 \tag{5.7}$$

which can be re-arranged to be:

$$n > \frac{\lambda_v}{C\mu_c} - \frac{1}{C} \tag{5.8}$$

Appendix C: Proof of Theorem 1

Applying the KKT conditions to the inequalities constraints of (2.10), we get:

$$\begin{aligned}
&\alpha_i^* \left(\lambda_v \left(p_{i-1}q_{i-1}^* - p_i q_i^*\right) + R^* - \lambda_v p_{i-1} + \lambda_c^{(i)}\right) = 0 \qquad i = 1, \ldots, n-1 \\
&\alpha_n^* \left(\lambda_v \left(p_{n-1}q_{n-1}^* - p_0 q_0^*\right) + R^* - \lambda_v p_{n-1} + \lambda_c^{(n)}\right) = 0 \\
&\beta_0^* \left(\sum_{i=0}^{n-1} \lambda_v \left(p_i - p_i q_i^*\right) - C\left(n\mu_c\right)\right) = 0 \\
&\beta_1^* \left(\lambda_v p_0 q_0^* - \mu_c\right) = 0 \\
&\gamma_i^* \left(q_i^* - 1\right) = 0 \qquad i = 0, \ldots, n-1 \\
&\omega_i^* q_i^* = 0 \qquad\qquad i = 0, \ldots, n-1 \\
&\omega_n^* R^* = 0
\end{aligned} \tag{5.9}$$

Likewise, applying the KKT conditions to the Lagrangian function in (2.11), and knowing that the gradient of the Lagrangian function goes to 0 at the optimal solution, we get the following set of equalities:

$$\begin{aligned}
&\lambda_v p_i \left(\alpha_{i+1}^* - \alpha_i^*\right) = \omega_i^* - \gamma_i^* \qquad i = 1, \ldots, n-1 \\
&\lambda_v p_0 \left(\alpha_1^* - \alpha_n^*\right) = \omega_0^* - \gamma_0^* \\
&\sum_{i=1}^{n-1} \alpha_i^* = 1
\end{aligned} \tag{5.10}$$

From Burke's theorem on the stability condition of the queues, the constraints on the charging queues are strict inequalities and the constraints on R should also be strictly larger than 0. Combining the Burke's theorem and the equations on (5.9), we find that $\beta_0^* = \beta_1^* = 0$ and $\omega_n^* = 0$.

Knowing that the gradient of the Lagrangian goes to 0 at the optimal solutions, we get the system of equalities given by (5.10). The fact that $\beta_i^* = 0$ and $\omega_n^* = 0$ explains the absence of β_i^* and ω_n^* in (2.12) The result given by multiplying the first equality in (5.10) by

q_i^* and the second equality by q_0^* combined with the last three equalities given by (5.9) gives:

$$\begin{aligned} &\lambda_v p_i \left(\alpha_{i+1}^* - \alpha_i^*\right) q_i^* = -\gamma_i^* \qquad i = 1, \ldots, n-1 \\ &\lambda_v p_0 \left(\alpha_1^* - \alpha_n^*\right) q_0^* = -\gamma_0^* \\ &\sum_{i=1}^{n-1} \alpha_i^* = 1 \end{aligned} \tag{5.11}$$

(5.11) Inserted in the fifth equality in (5.9) gives:

$$\begin{aligned} &\lambda_v p_i \left(\alpha_{i+1}^* - \alpha_i^*\right) \left(q_i^* - 1\right) q_i^* = 0 \qquad i = 1, \ldots, n-1 \\ &\lambda_v p_0 \left(\alpha_1^* - \alpha_n^*\right) \left(q_0^* - 1\right) q_0^* = 0 \\ &\sum_{i=1}^{n-1} \alpha_i^* = 1 \end{aligned} \tag{5.12}$$

From (5.12) we have $0 < q_0^* < 1$ only if $\alpha_1^* = \alpha_n^*$ And $0 < q_i^* < 1$ only if $\alpha_{i+1}^* = \alpha_i^*$ Since $0 \leq q_i^* \leq 1$ then these equalities may not always be true

if $\alpha_1^* > \alpha_n^*$ and we know that $\gamma_0^* \geq 0$ then $\gamma_0^* = 0$ which gives $q_0^* \neq 1$ and $q_0^* = 0$

if $\alpha_{i+1}^* > \alpha_i^*$ and we know that $\gamma_i^* \geq 0$ then $\gamma_i^* = 0$ which gives $q_i^* \neq 1$ and $q_i^* = 0$

if $\alpha_1^* < \alpha_n^*$ then $\gamma_0^* > 0$ (it cannot be 0 because this will contradict with the value of q_i), which implies that $q_0^* = 1$

if $\alpha_{i+1}^* < \alpha_i^*$ then $\gamma_i^* > 0$ (it cannot be 0 because this contradicts with the value of q_i), which implies that $q_i^* = 1$

Otherwise, if $\alpha_1^* = \alpha_n^* \neq 0$ (they cannot be equal to 0 at the same time, which means that $q_0 = 1$, and we know in advance that this cannot be the case here), we have $q_1^* = \frac{p_0 q_0^*}{p_1} - \frac{\lambda_v p_0 - \lambda_c^{(1)} - R^*}{\lambda_v p_1}$ and $q_{n-1}^* = \frac{p_0 q_0^*}{p_{n-1}} - \frac{\lambda_v p_0 - \lambda_c^{(n)} - R^*}{\lambda_v p_{n-1}}$

Finally, if $\alpha_{i+1}^* = \alpha_i^* \neq 0$ (they cannot be equal to 0 at the same time, which means that $q_i = 1$, and we know in advance that this cannot be the case here), we have $q_i^* = \frac{p_{i-1} q_{i-1}^*}{p_i} - \frac{\lambda_v p_{i-1} - \lambda_c^{(i)} - R^*}{\lambda_v p_i}$ and $q_{i+1}^* = \frac{p_i q_i^*}{p_{i+1}} - \frac{\lambda_v p_i - \lambda_c^{(i+1)} - R^*}{\lambda_v p_{i+1}}$

Appendix D: Proof of Theorem 2

To prove this theorem, we first start by putting the problem on the standard linear programming form as follows:

$$
\begin{aligned}
&\underset{q_0,q_1,\ldots,q_{n-1}}{\text{minimize}} \; -R \\
&\text{subject to} \\
&\lambda_v \left(p_{i-1}q_{i-1} - p_i q_i\right) + R \leq \lambda_v p_{i-1} - \lambda_c^{(i)},\ i = 1,\ldots,n-1 \\
&\lambda_v \left(p_{n-1}q_{n-1} - p_0 q_0\right) + R \leq \lambda_v p_{n-1} - \lambda_c^{(n)} \\
&-\lambda_v \sum_{i=0}^{n-1} p_i q_i^* < C\left(n\mu_c\right) - \lambda_v \\
&\lambda_v p_0 q_0 < \mu_c \\
&q_i \leq 1 \qquad\qquad i = 0,\ldots,n-1 \\
&-q_i \leq 0 \qquad\qquad i = 0,\ldots,n-1 \\
&-R < 0 \\
&\sum_{i=0}^{n-1} p_i = 1 \qquad 0 < p_i < 1 \qquad i = 0,\ldots,n-1
\end{aligned}
\tag{5.13}
$$

Writing the problem on its matrix form, we get:

$$
\begin{aligned}
&\underset{X}{\text{minimize}} \quad \mathbf{c}^T\mathbf{x} \\
&\text{subject to} \quad \mathbf{A}\mathbf{x} \preceq \mathbf{b}
\end{aligned}
\tag{5.14}
$$

where:

$$\mathbf{x}_{(n+1\times 1)} = \begin{pmatrix} q_0 \\ q_1 \\ \vdots \\ q_{n-1} \\ R \end{pmatrix} \quad \mathbf{c}_{(n+1\times 1)} = \begin{pmatrix} 0 \\ 0 \\ 0 \\ \vdots \\ -1 \end{pmatrix} \mathbf{b}_{(3n+4\times 1)} = \begin{pmatrix} \lambda_v p_0 - \lambda_c^{(1)} \\ \vdots \\ \lambda_v p_{n-1} - \lambda_c^{(n)} \\ C\left(n\mu_c\right) - \lambda_v \\ \mu_c \\ 1 \\ \vdots \\ 1 \\ \infty \\ 0 \\ \vdots \\ 0 \end{pmatrix} \tag{5.15}$$

$$\mathbf{A}_{(3n+4\times n+1)} = \begin{pmatrix} \lambda_v p_0 & -\lambda_v p_1 & 0 & \dots & 0 & 1 \\ 0 & \lambda_v p_1 & -\lambda_v p_2 & \dots & 0 & 1 \\ \vdots & \ddots & \ddots & \ddots & \ddots & \vdots \\ 0 & \dots & 0 & \lambda_v p_{n-2} & -\lambda_v p_{n-1} & 1 \\ -\lambda_v p_0 & 0 & \dots & \dots & \lambda_v p_{n-1} & 1 \\ -\lambda_v p_0 & -\lambda_v p_1 & \dots & \dots & -\lambda_v p_{n-1} & 0 \\ \lambda_v p_0 & 0 & \dots & \dots & \dots & 0 \\ & & I_{n+1} & & & \\ & & -I_{n+1} & & & \end{pmatrix} \tag{5.16}$$

The matrix form of the Lagrangian function can be thus expressed as: Lagrangian:

$$L(\mathbf{x}, \boldsymbol{\nu}) = \mathbf{c}^T\mathbf{x} + \boldsymbol{\nu}^T(\mathbf{A}\mathbf{x} - \mathbf{b}) = -\mathbf{b}^T + \left(\mathbf{A}^T\boldsymbol{\nu} + \mathbf{c}\right)^T\mathbf{x} \tag{5.17}$$

where $\boldsymbol{\nu}$ is the vector of the dual variables or Lagrange multipliers vector associated with the problem 5.14. Each element ν_i of $\boldsymbol{\nu}$ is the Lagrange multiplier associated with the i-th inequality constraint $\mathbf{a}_i\mathbf{x} - b_i \leq 0$, where $\mathbf{a}_i$ and b_i are the the i-th row and and i-th element of matrix $\mathbf{A}$ and vector $\mathbf{b}$, respectively. In fact $\boldsymbol{\nu}$ is the vector that includes all the vectors $\boldsymbol{\alpha}$, $\boldsymbol{\beta}$, $\boldsymbol{\gamma}$, $\boldsymbol{\omega}$ as follows:

$$\boldsymbol{\nu}^T_{(1\times 3n+4)} = \begin{pmatrix} \alpha_1 & \dots & \alpha_n & \beta_0 & \beta_1 & \gamma_0 & \dots & \gamma_n & \omega_0 & \dots & \omega_n \end{pmatrix} \tag{5.18}$$

We will used this combined notation for ease and clarity of notation.

The Lagrange dual function is expressed as:

$$g(\boldsymbol{\nu}) = \inf_{\mathbf{x}} L(\mathbf{x}, \boldsymbol{\nu}) = -\mathbf{b}^T\boldsymbol{\nu} + \inf_{\mathbf{x}} \left(\mathbf{A}^T\boldsymbol{\nu} + \mathbf{c}\right)^T\mathbf{x} \tag{5.19}$$

The solution for this function is easily determined analytically, since a linear function is bounded below only when it is identically zero. Thus, $g(\boldsymbol{\nu}) = -\infty$ except when $\mathbf{A}^T\boldsymbol{\nu} + \mathbf{c} = \mathbf{0}$, where $\mathbf{0}$ is the all zero vector. Consequently, we have:

$$g(\boldsymbol{\nu}) = \begin{cases} -\mathbf{b}^T\boldsymbol{\nu} & \mathbf{A}^T\boldsymbol{\nu} + \mathbf{c} = \mathbf{0} \\ -\infty & \text{ortherwise} \end{cases} \tag{5.20}$$

For each $\nu \succeq \mathbf{0}$ (i.e., $\nu_i \geq 0 \ \forall \ i$), the Lagrange dual function gives us a lower bound on the optimal value of the original optimization problem. This leads to a new equivalent

optimization problem, which is the dual problem:

$$\begin{aligned} \max_{\boldsymbol{\nu}} \quad & g(\boldsymbol{\nu}) = -\mathbf{b}^T \boldsymbol{\nu} \\ \text{subject to} \quad & \mathbf{A}^T \boldsymbol{\nu} + \mathbf{c} = \mathbf{0} \\ & \boldsymbol{\nu} \succeq \mathbf{0} \end{aligned} \tag{5.21}$$

Applying Slater's Theorem for duality qualification, and since strong duality holds for the considered optimization problem, then solving the dual problem gives the exact optimal solution for the primal problem. This is described by the equality:

$$g(\boldsymbol{\nu}^*) = -\mathbf{b}^T \boldsymbol{\nu}^* = \mathbf{c}^T \mathbf{x}^* = -R^* \tag{5.22}$$

By expanding on the values of $\mathbf{b}$ and $\boldsymbol{\nu}$ in the above equation, the optimal value of R^* can be expressed as:

$$R^* = \sum_{i=1}^{n} \left(\lambda_v p_{i-1} - \lambda_c^{(i)} \right) \alpha_i^* + \sum_{i=0}^{n-1} \gamma_i^* \tag{5.23}$$

Appendix E: Proof of Lemma 3

After performing the suggested substitutions in the lemma statement, the function f can be expressed as:

$$\begin{aligned} f\left(q_0, q_1, \ldots, q_{n-1}\right) &= \frac{1}{n}\sum_{i=1}^{n}\frac{1}{\lambda_v^{(i)} - \lambda_c^{(i)}} \\ &= \frac{1}{n}\sum_{i=1}^{n-1}\frac{1}{\lambda_v\left(p_{i-1} - p_{i-1}q_{i-1} + p_i q_i\right) - \lambda_c^{(i)}} + \frac{1}{n\left(\lambda_v\left(p_{n-1} - p_{n-1}q_{n-1} + p_0 q_0\right) - \lambda_c^{(n)}\right)} \end{aligned} \tag{5.24}$$

In order to prove that the function f is a convex, we need to first show that it is continuous and second order differentiable which is the case of our function because it is a sum of continuous and second order differentiable functions. Moreover, since f is a multi-variable function, we need to show that its Hessian matrix is positive semi-definite. Let H be the Hessian matrix of f such that:

$$H_{i,j} = \frac{\partial^2 f}{\partial q_i \partial q_j} \qquad i, j = 0, \ldots, n-1 \tag{5.25}$$

We notice that the Hessian matrix is a symmetric matrix because

$$\frac{\partial^2 f}{\partial q_j \partial q_i} = \frac{\partial^2 f}{\partial q_i \partial q_j} \qquad \forall\ i, j \tag{5.26}$$

which means that:

$$H_{i,j} = H_{j,i} \qquad \forall\ i, j \tag{5.27}$$

The calculation of the terms in the Hessian matrix leads to the following results:

$$
\begin{aligned}
\frac{\partial^2 f}{\partial^2 q_0} &= \frac{2\lambda_v^2 p_0^2}{\left(\lambda_v\left(p_0 - p_0 q_0 + p_1 q_1\right) - \lambda_c^{(1)}\right)^3} + \frac{2\lambda_v^2 p_0^2}{\left(\lambda_v\left(p_{n-1} - p_{n-1} q_{n-1} + p_0 q_0\right) - \lambda_c^{(n)}\right)^3} \\
\frac{\partial^2 f}{\partial^2 q_i} &= \frac{2\lambda_v^2 p_i^2}{\left(\lambda_v\left(p_{i-1} - p_{i-1} q_{i-1} + p_i q_i\right) - \lambda_c^{(i)}\right)^3} + \frac{2\lambda_v^2 p_i^2}{\left(\lambda_v\left(p_i - p_i q_i + p_{i+1} q_{i+1}\right) - \lambda_c^{(i+1)}\right)^3} \quad i = 1, \ldots, n-2 \\
\frac{\partial^2 f}{\partial^2 q_{n-1}} &= \frac{2\lambda_v^2 p_{n-1}^2}{\left(\lambda_v\left(p_{n-2} - p_{n-2} q_{n-2} + p_{n-1} q_{n-1}\right) - \lambda_c^{(n-1)}\right)^3} + \frac{2\lambda_v^2 p_{n-1}^2}{\left(\lambda_v\left(p_{n-1} - p_{n-1} q_{n-1} + p_0 q_0\right) - \lambda_c^{(n)}\right)^3} \\
\frac{\partial^2 f}{\partial^2 q_{i-1} q_i} &= \frac{-2\lambda_v^2 p_{i-1} p_i}{\left(\lambda_v\left(p_{i-1} - p_{i-1} q_{i-1} + p_i q_i\right) - \lambda_c^{(i)}\right)^3} \qquad i = 1, \ldots, n-1 \\
\frac{\partial^2 f}{\partial^2 q_i q_j} &= 0 \qquad j > i+1,\ i, j = 0, \ldots, n-1 \\
\frac{\partial^2 f}{\partial^2 q_{n-1} q_0} &= \frac{-2\lambda_v^2 p_0 p_{n-1}}{\left(\lambda_v\left(p_{n-1} - p_{n-1} q_{n-1} + p_0 q_0\right) - \lambda_c^{(n)}\right)^3}
\end{aligned}
\tag{5.28}
$$

Let $\boldsymbol{x} = [x_i]$ be an $n \times 1$ vector such that $0 \leq x_i \leq 1 \ \forall \ i$ since our variables q_i which on the function depends are varies that range $q_i \in [0, 1]$. To prove that $\mathbf{H}$ is positive semi-definite, it should satisfy the following condition:

$$
\mathbf{x}^T \mathbf{H} \mathbf{x} \geq 0 \tag{5.29}
$$

$$
\mathbf{x}^T \mathbf{H} = \begin{cases}
x_0 \frac{\partial^2 f}{\partial^2 q_0} + x_1 \frac{\partial^2 f}{\partial^2 q_0 q_1} + x_{n-1} \frac{\partial^2 f}{\partial^2 q_0 q_{n-1}} \\
x_{i-1} \frac{\partial^2 f}{\partial^2 q_{i-1} q_i} + x_i \frac{\partial^2 f}{\partial^2 q_i} + x_{i+1} \frac{\partial^2 f}{\partial^2 q_{i+1} q_i} \\
\qquad\qquad\qquad\qquad\qquad\qquad i = 1 \ldots n-2 \\
x_0 \frac{\partial^2 f}{\partial^2 q_0 q_{n-1}} + x_{n-2} \frac{\partial^2 f}{\partial^2 q_{n-1} q_{n-2}} + x_{n-1} \frac{\partial^2 f}{\partial^2 q_{n-1}}
\end{cases} \tag{5.30}
$$

Multiplying (5.30) by the vector $\mathbf{x}$ gives:

$$\mathbf{x}^T\mathbf{H}\mathbf{x} = x_0\left(x_0\frac{\partial^2 f}{\partial^2 q_0} + x_1\frac{\partial^2 f}{\partial^2 q_0 q_1} + x_{n-1}\frac{\partial^2 f}{\partial^2 q_0 q_{n-1}}\right) + \sum_{i=1}^{n-2} x_i\left(x_{i-1}\frac{\partial^2 f}{\partial^2 q_{i-1}q_i} + x_i\frac{\partial^2 f}{\partial^2 q_i} + x_{i+1}\frac{\partial^2 f}{\partial^2 q_{i+1}q_i}\right) + x_{n-1}\left(x_0\frac{\partial^2 f}{\partial^2 q_0 q_{n-1}} + x_{n-2}\frac{\partial^2 f}{\partial^2 q_{n-1}q_{n-2}} + x_{n-1}\frac{\partial^2 f}{\partial^2 q_{n-1}}\right) \tag{5.31}$$

Simplifying (5.31) gives:

$$\mathbf{x}^T\mathbf{H}\mathbf{x} = \sum_{i=0}^{n-1} x_i^2\frac{\partial^2 f}{\partial^2 q_i} + 2\sum_{i=1}^{n-1} x_i x_{i-1}\frac{\partial^2 f}{\partial^2 q_{i-1}q_i} + 2x_0 x_{n-1}\frac{\partial^2 f}{\partial^2 q_{n-1}q_0} \tag{5.32}$$

Substitute (5.28) in (5.32), we get:

$$\mathbf{x}^T\mathbf{H}\mathbf{x} = \sum_{i=1}^{n-1}\frac{2\lambda_v^2\left(p_i x_i - p_{i-1}x_{i-1}\right)^2}{\left(\lambda_v\left(p_{i-1} - p_{i-1}q_{i-1} + p_i q_i\right) - \lambda_c^{(i)}\right)^3} + \frac{2\lambda_v^2\left(p_0 x_0 - p_{n-1}x_{n-1}\right)^2}{\left(\lambda_v\left(p_{n-1} - p_{n-1}q_{n-1} + p_0 q_0\right) - \lambda_c^{(n)}\right)^3} \tag{5.33}$$

We can see clearly that $\mathbf{x}^T\mathbf{H}\mathbf{x} \geq 0$ because it is a sum of positive terms. Consequently, $\mathbf{H}$ is positive semi-definite, thus making f a convex function.

Appendix F: Proof of Theorem 3

Applying the KKT conditions to the inequalities constraints of the problem (2.15), we get:

$$\begin{aligned}
&\alpha_i^* \left(\lambda_c^{(i)} - \lambda_v \left(p_{i-1} - p_{i-1}q_{i-1}^* + p_i q_i^*\right)\right) = 0 \quad i = 1, \ldots, n-1 \\
&\alpha_n^* \left(\lambda_c^{(n)} - \lambda_v \left(p_{n-1} - p_{n-1}q_{n-1}^* + p_0 q_0^*\right)\right) = 0 \\
&\beta_0^* \left(\sum_{i=0}^{n-1} \lambda_v \left(p_i - p_i q_i^*\right) - C\left(n\mu_c\right)\right) = 0 \\
&\beta_1^* \left(\lambda_v p_0 q_0^* - \mu_c\right) = 0 \\
&\gamma_i^* \left(q_i^* - 1\right) = 0 \qquad\qquad i = 0, \ldots, n-1 \\
&\omega_i^* q_i^* = 0 \qquad\qquad i = 0, \ldots, n-1
\end{aligned} \tag{5.34}$$

From Burke's theorem on the stability condition of queues, the constraints on the customers' queues and the charging queues are strict inequalities. Combining Burke's theorem with the equations in (5.34), we find that $\beta_0^* = \beta_1^* = 0$ and $\alpha_i^* = 0 \; \forall \; i$. Applying the KKT conditions to the Lagrangian function in (2.17), and knowing that the gradient of the Lagrangian function goes to 0 at the optimal solution, we get the following set of equalities:

$$\begin{aligned}
&\frac{\lambda_v p_0}{n}\left(\frac{1}{\left(\lambda_v\left(p_{n-1} - p_{n-1}q_{n-1}^* + p_0 q_0^*\right) - \lambda_c^{(n)}\right)^2} - \frac{1}{\left(\lambda_v\left(p_0 - p_0 q_0^* + p_1 q_1^*\right) - \lambda_c^{(1)}\right)^2}\right) + \gamma_0^* - \omega_0^* = 0 \\
&\frac{\lambda_v p_i}{n}\left(\frac{1}{\left(\lambda_v\left(p_{i-1} - p_{i-1}q_{i-1}^* + p_i q_i^*\right) - \lambda_c^{(i)}\right)^2} - \frac{1}{\left(\lambda_v\left(p_i - p_i q_i^* + p_{i+1} q_{i+1}^*\right) - \lambda_c^{(i+1)}\right)^2}\right) + \gamma_i^* - \omega_i^* = 0 \\
&\qquad\qquad i = 1 \ldots n-2 \\
&\frac{\lambda_v p_{n-1}}{n}\left(\frac{1}{\left(\lambda_v\left(p_{n-2} - p_{n-2}q_{n-2}^* + p_{n-1} q_{n-1}^*\right) - \lambda_c^{(n-1)}\right)^2} - \frac{1}{\left(\lambda_v\left(p_{n-1} - p_{n-1}q_{n-1}^* + p_0 q_0^*\right) - \lambda_c^{(n)}\right)^2}\right) \\
&+ \gamma_{n-1}^* - \omega_{n-1}^* = 0
\end{aligned} \tag{5.35}$$

The fact that $\beta_i^* = 0$ and $\omega_i^* = 0$ explains the absence of β_i^* and ω_i^* in (5.35). Multiplying the first equality in (5.35) by q_0^*, the second by q_i^*, and the third by q_{n-1}^* gives:

$$\gamma_0^* = \frac{\lambda_v p_0}{n} q_0^* \left(\frac{1}{\left(\lambda_v \left(p_0 - p_0 q_0^* + p_1 q_1^*\right) - \lambda_c^{(1)}\right)^2} - \frac{1}{\left(\lambda_v \left(p_{n-1} - p_{n-1} q_{n-1}^* + p_0 q_0^*\right) - \lambda_c^{(n)}\right)^2} \right)$$

$$\gamma_i^* = \frac{\lambda_v p_i}{n} qi^* \left(\frac{1}{\left(\lambda_v \left(p_i - p_i q_i^* + p_{i+1} q_{i+1}^*\right) - \lambda_c^{(i+1)}\right)^2} - \frac{1}{\left(\lambda_v \left(p_{i-1} - p_{i-1} q_{i-1}^* + p_i q_i^*\right) - \lambda_c^{(i)}\right)^2} \right) \quad i = 1 \ldots n$$

$$\gamma_{n-1}^* = \frac{\lambda_v p_{n-1}}{n} q_{n-1}^* \left(\frac{1}{\left(\lambda_v \left(p_{n-1} - p_{n-1} q_{n-1}^* + p_0 q_0^*\right) - \lambda_c^{(n)}\right)^2} - \frac{1}{\left(\lambda_v \left(p_{n-2} - p_{n-2} q_{n-2}^* + p_{n-1} q_{n-1}^*\right) - \lambda_c^{(n-1)}\right)^2} \right) \tag{5.36}$$

Inserting (5.36) in the fifth equality of (5.35) gives:

$$\left(q_0^* - 1\right) q_0^* \left(\frac{1}{\left(\lambda_v \left(p_0 - p_0 q_0^* + p_1 q_1^*\right) - \lambda_c^{(1)}\right)^2} - \frac{1}{\left(\lambda_v \left(p_{n-1} - p_{n-1} q_{n-1}^* + p_0 q_0^*\right) - \lambda_c^{(n)}\right)^2} \right) = 0$$

$$\left(q_i^* - 1\right) qi^* \left(\frac{1}{\left(\lambda_v \left(p_i - p_i q_i^* + p_{i+1} q_{i+1}^*\right) - \lambda_c^{(i+1)}\right)^2} - \frac{1}{\left(\lambda_v \left(p_{i-1} - p_{i-1} q_{i-1}^* + p_i q_i^*\right) - \lambda_c^{(i)}\right)^2} \right) = 0$$

$$i = 1 \ldots n-2$$

$$\left(q_{n-1}^* - 1\right) q_{n-1}^* \left(\frac{1}{\left(\lambda_v \left(p_{n-1} - p_{n-1} q_{n-1}^* + p_0 q_0^*\right) - \lambda_c^{(n)}\right)^2} - \frac{1}{\left(\lambda_v \left(p_{n-2} - p_{n-2} q_{n-2}^* + p_{n-1} q_{n-1}^*\right) - \lambda_c^{(n-1)}\right)^2} \right) \tag{5.37}$$

From (5.34), we have $0 < q_i^* < 1 \; \forall \; i$ only if $\gamma_i^* = 0$ and $\omega_i^* = 0$. Since $0 \leq q_i^* \leq 1$, the above result may not always be true. From (5.34) and (5.37), we finally get:

$$q_i^* = \begin{cases} 0 & \text{if } \omega_i^* \neq 0 \\ \\ 1 & \text{if } \gamma_i^* \neq 1 \end{cases} \qquad i = 0, \ldots, n-1$$

Otherwise, we have:

$$q_0^* = \frac{\lambda_v \left(p_0 + p_1 q_1^* - p_{n-1} + p_{n-1} q_{n-1}^*\right) - \lambda_c^{(1)} + \lambda_c^{(n)}}{2\lambda_v p_0} \tag{5.38}$$

$$q_i^* = \frac{\lambda_v \left(p_i + p_{i+1} q_{i+1}^* - p_{i-1} + p_{i-1} q_{i-1}^*\right) - \lambda_c^{(i+1)} + \lambda_c^{(i)}}{2\lambda_v p_i} \quad i = 1, \ldots, n-2$$

$$q_{n-1}^* = \frac{\lambda_v \left(p_{n-1} + p_0 q_0^* - p_{n-2} + p_{n-2} q_{n-2}^*\right) - \lambda_c^{(n)} + \lambda_c^{(n-1)}}{2\lambda_v p_{n-1}}$$

Proof of Lemma 4

From (2.2) and (3.3) we have

$$\begin{aligned} \lambda_c^{(i)} + \frac{1}{T} &\leq \lambda_v(p_{i-1}\overline{q}_{i-1} + p_i q_i),\ i = 1, \ldots, n-1. \\ \lambda_c^{(n)} + \frac{1}{T} &\leq \lambda_v(p_{n-1}\overline{q}_{n-1} + p_0 q_0),\ i = n \end{aligned} \tag{5.39}$$

The summation of all the inequalities in (5.39) gives a new inequality

$$\sum_{i=1}^{n} \lambda_c^{(i)} + \frac{n}{T} \leq \lambda_v[\sum_{i=1}^{n-1}(p_{i-1}\overline{q}_{i-1} + p_i q_i) + (p_{n-1}\overline{q}_{n-1} + p_0 q_0)] \tag{5.40}$$

$$\sum_{i=1}^{n} \lambda_c^{(i)} + \frac{n}{T} \leq \lambda_v[p_0\overline{q}_0 + p_1 q_1 + p_1\overline{q}_1 + ... + p_{n-1}\overline{q}_{n-1} + p_0 q_0] \tag{5.41}$$

We have $\overline{q}_i + q_i$ so $p_i\overline{q}_i + p_i q_i = p_i$

$$\sum_{i=1}^{n} \lambda_c^{(i)} + \frac{n}{T} \leq \lambda_v(p_0 + p_1 + p_2 + ... + p_{n-1}) \tag{5.42}$$

We have $\sum_{i=0}^{n-1} p_i = 1$ so $\sum_{i=1}^{n} \lambda_c^{(i)} + \frac{n}{T} \leq \lambda_v$

Proof of Lemma 5

The summation of the inequalities given by (2.4) $\forall\ i = \{0, \ldots, n\}$ gives the following inequality :

$$\lambda_v \sum_{i=0}^{n-1} p_i - \lambda_v \sum_{i=0}^{n-1} p_i q_i + \lambda_v p_0 q_0 < C(n\mu_c) + \mu_c \tag{5.43}$$

Since $\sum_{i=0}^{n-1} p_i = 1$ (because $p_n = 0$ as described in Section 2), we get:

$$\lambda_v - \lambda_v \sum_{i=1}^{n-1} p_i q_i < \mu_c(Cn + 1) \tag{5.44}$$

In the worst case, all the vehicles will be directed to partially charge before serving, which means that always $q_i = 0$. Therefore, we get:

$$Cn > \frac{\lambda_v}{\mu_c} - 1\ , \tag{5.45}$$

which can be re-arranged to be:

$$n > \frac{\lambda_v}{C\mu_c} - \frac{1}{C} \tag{5.46}$$

From equation (5.46) and equation (3.4) we have

$$n > \frac{\lambda_v}{C\mu_c} - \frac{1}{C} \geq \frac{\sum_{i=1}^{n} \lambda_c^{(i)} + \frac{n}{T}}{C\mu_c} - \frac{1}{C} \tag{5.47}$$

By simplifying equation (5.47) we get

$$n \geq T\frac{\sum_{i=1}^{n} \lambda_c^{(i)} - \mu_c}{TC\mu_c - 1} \tag{5.48}$$

Proof of Theorem 4

Applying the KKT conditions to the inequalities constraints of (3.5), we get:

$$\begin{aligned}
&\alpha_i^*(\lambda_v^*(p_{i-1}q_{i-1}^* - p_i q_i^* - p_{i-1}) + \frac{1}{T} + \lambda_c^{(i)}) = 0 \\
&i = 1, \ldots, n-1. \\
&\alpha_n^*(\lambda_v^*(p_{n-1}q_{n-1}^* - p_0 q_0^* - p_{n-1}) + \frac{1}{T} + \lambda_c^{(n)}) = 0. \\
&\beta_0^*(\sum_{i=0}^{n-1} \lambda_v(p_i - p_i q_i^*) - C(n\mu_c) + \epsilon_0) = 0. \\
&\beta_1^*(\lambda_v p_0 q_0^* - \mu_c + \epsilon_1) = 0 \\
&\gamma_i^*(q_i^* - 1) = 0,\ i = 0, \ldots, n-1. \\
&\omega_i^* q_i^* = 0,\ i = 0, \ldots, n-1. \\
&\omega_n^*(\lambda_v^* - (\sum_{i=1}^{n} \lambda_c^{(i)} + \frac{n}{T})) = 0.
\end{aligned} \tag{5.49}$$

Likewise, applying the KKT conditions to the Lagrangian function in (3.6), and knowing that the gradient of the Lagrangian function goes to 0 at the optimal solution, we get the following set of equalities:

$$\begin{aligned}
&\lambda_v^* p_i(\alpha_{i+1}^* - \alpha_i^* - \beta_0^*) = \omega_i^* - \gamma_i^*,\ i = 1, \ldots, n-1. \\
&\lambda_v^* p_0(\alpha_1^* - \alpha_n^* - \beta_0^* + \beta_1^*) = \omega_0^* - \gamma_0^* \\
&\sum_{i=1}^{n-1} \alpha_i^*(p_{i-1}q_{i-1}^* - p_i q_i^* - p_{i-1}) + \alpha_n^*(p_{n-1}q_{n-1}^* \\
&- p_0 q_0^* - p_{n-1}) + \beta_0^*(\sum_{i=0}^{n-1}(p_i - p_i q_i^*)) + \beta_1^* p_0 q_0^* - \omega_n^* + 1 = 0
\end{aligned} \tag{5.50}$$

Knowing that the gradient of the Lagrangian goes to 0 at the optimal solutions, we get the system of equalities given by (5.50). multiplying the first equality in (5.50) by q_i^* and the second equality by q_0^* and the third equality by λ_v^*combined with the equalities given by

(5.49) gives :

$$\begin{aligned}
&\lambda_v^* p_i q_i^* (\alpha_{i+1}^* - \alpha_i^* - \beta_0^*) = -\gamma_i^*,\ i = 1, \ldots, n-1. \\
&\lambda_v^* p_0 q_0^* (\alpha_1^* - \alpha_n^* - \beta_0^* + \beta_1^*) = -\gamma_0^* \\
&\lambda_v^* - \sum_{i=1}^{n} \alpha_i^* (\lambda_c^{(i)} + \frac{1}{T}) + \beta_0^* (Cn\mu_c - \epsilon_0) + \beta_1^* (\mu_c - \epsilon_1) \\
&- \omega_n^* (\sum_{i=1}^{n} \lambda_c^{(i)} + \frac{n}{T}) = 0
\end{aligned} \tag{5.51}$$

(5.51) Inserted in the fifth equality in (5.49) gives :

$$\begin{aligned}
&\lambda_v^* p_i (\alpha_{i+1}^* - \alpha_i^* - \beta_0^*)(q_i^* - 1) q_i^* = 0,\ i = 1, \ldots, n-1. \\
&\lambda_v^* p_0 (\alpha_1^* - \alpha_n^* - \beta_0^* + \beta_1^*)(q_0^* - 1) q_0^* = 0 \\
&\lambda_v^* = \sum_{i=1}^{n} \alpha_i^* (\lambda_c^{(i)} + \frac{1}{T}) - \beta_0^* (Cn\mu_c - \epsilon_0) - \beta_1^* (\mu_c - \epsilon_1) \\
&+ \omega_n^* (\sum_{i=1}^{n} \lambda_c^{(i)} + \frac{n}{T})
\end{aligned} \tag{5.52}$$

From (5.52) we have $0 < q_0^* < 1$ only if $\alpha_{i+1}^* - \alpha_i^* - \beta_0^* = 0$ And $0 < q_i^* < 1$ only if $\alpha_1^* - \alpha_n^* - \beta_0^* + \beta_1^* = 0$ Since $0 \leq q_i^* \leq 1$ then these equalities may not always be true

if $\alpha_1^* - \alpha_n^* - \beta_0^* + \beta_1^* > 0$ and we know that $\gamma_0^* \geq 0$ then $\gamma_0^* = 0$ which gives $q_0^* \neq 1$ and $q_0^* = 0$.

if $\alpha_{i+1}^* - \alpha_i^* - \beta_0^* > 0$ and we know that $\gamma_i^* \geq 0$ then $\gamma_i^* = 0$ which gives $q_i^* \neq 1$ and $q_i^* = 0$

if $\alpha_1^* - \alpha_n^* - \beta_0^* + \beta_1^* < 0$ then $\gamma_0^* > 0$ (it cannot be 0 because this will contradict with the value of q_i), which implies that $q_0^* = 1$.

if $\alpha_{i+1}^* - \alpha_i^* - \beta_0^* < 0$ then $\gamma_i^* > 0$ (it cannot be 0 because this contradicts with the value of q_i), which implies that $q_i^* = 1$

We have also from the KKT conditions given by equation in in (5.49) that says either the Lagrangian coefficient is 0 or its the associated inequality is an equality:

if $\beta_1^* \neq 0$ we have $q_0^* = \frac{\mu_c}{\lambda_v^* p_0}$

if $\alpha_n^* \neq 0$ we have $q_0^* = \frac{p_{n-1} q_{n-1}^* - p_{n-1}}{p_0} + \frac{\lambda_c^{(n)} + \frac{1}{T}}{\lambda_v p_0}$

if $\alpha_i^* \neq 0$, we have $q_i^* = \frac{p_{i-1}q_{i-1}^* - p_{i-1}}{p_i} + \frac{\lambda_c^{(i)} + \frac{1}{T}}{\lambda_v p_i}$

for $i = 1, \ldots, n-1$

Otherwise by the Lagrangian relaxation:

$q_i^* = \zeta_i(\alpha^*, \beta^*, \gamma^*, \lambda_v^*, q^*)$ for $i = 1, \ldots, n-1$

Where $\zeta_i(\alpha^*, \beta^*, \gamma^*, \lambda_v^*, q^*)$ is the solution that that maximize the function $\inf_{\mathbf{q}} L(\mathbf{q}, \alpha^*, \beta^*, \gamma^*, \lambda_v^*)$

Now in order to find the expression of λ_v^* we first look at the last equation in (5.49). From there we can say that if $\omega_n^* \neq 0$ then $\lambda_v^* = \sum_{i=1}^n \lambda_c^{(i)} + \frac{n}{T}$

Otherwise from the third equation in (5.52) if $\omega_n^* = 0$ then $\lambda_v^* = \sum_{i=1}^n \alpha_i^*(\lambda_c^{(i)} + \frac{1}{T}) - \beta_0^*(Cn\mu_c - \epsilon_0) - \beta_1^*(\mu_c - \epsilon_1)$

Proof of Lemma 6

From (4.4) and (4.6) we have :

$$\begin{aligned}
&\lambda_c^{(i)} + R \leq \lambda_v \sum_{k=i}^{n-1}(p_{k-1} - p_{k-1}q_{k-1} + p_k q_k)\Pi_{ki} + \lambda_v(p_{n-1} - p_{n-1}q_{n-1} + p_0 q_0)\Pi_{ni},\ i = 1, \ldots, n-1 \\
&\lambda_c^{(n)} + R \leq \lambda_v(p_{n-1} - p_{n-1}q_{n-1} + p_0 q_0)\Pi_{nn}
\end{aligned} \tag{5.53}$$

The summation of all the inequalities in (5.53) gives a new inequality

$$\sum_{i=1}^{n} \lambda_c^{(i)} + nR \leq \sum_{i=1}^{n}\sum_{k=1}^{n} \lambda_v^{(k)}\Pi_{ki} \tag{5.54}$$

Which is equivalent to:

$$\sum_{i=1}^{n} \lambda_c^{(i)} + nR \leq \sum_{i=1}^{n} \lambda_v^{(i)} \sum_{k=1}^{i}\Pi_{ik} \tag{5.55}$$

Since We have $\sum_{j=1}^{i}\Pi_{ij} = 1,\ i = 1, \ldots, n$ then:

$$\sum_{i=1}^{n} \lambda_c^{(i)} + nR \leq \sum_{i=1}^{n} \lambda_v^{(i)} \tag{5.56}$$

From (4.1) and (4.2)

$$\sum_{i=1}^{n} \lambda_v^{(i)} = \sum_{i=1}^{n-1}(p_{i-1}\overline{q}_{i-1} + p_i q_i) + (p_{n-1}\overline{q}_{n-1} + p_0 q_0) \tag{5.57}$$

Since $\overline{q}_i + q_i = 1$ and we have $\sum_{i=0}^{n-1} p_i = 1$ then:

$$\sum_{i=1}^{n} \lambda_c^{(i)} + nR \leq \lambda_v \tag{5.58}$$

Proof of Theorem 5

Applying the KKT conditions to the inequalities constraints of (4.11), we get:

$$\alpha_i^*(\lambda_c^{(i)} + R^* - \lambda_v \sum_{k=i}^{n-1}(p_{k-1} - p_{k-1}q_{k-1}^* + p_k q_k^*)\Pi_{ki}^* - \lambda_v(p_{n-1} - p_{n-1}q_{n-1}^* + p_0 q_0^*)\Pi_{ni}^*) = 0 \; i = 1, \ldots, n -$$

$$\alpha_n^*(\lambda_c^{(n)} + R^* - \lambda_v(p_{n-1} - p_{n-1}q_{n-1}^* + p_0 q_0^*)\Pi_{nn}^*) = 0.$$

$$\beta_0^*(\sum_{i=0}^{n-1} \lambda_v(p_i - p_i q_i^*) - C(n\mu_c)) = 0.$$

$$\beta_1^*(\lambda_v p_0 q_0^* - \mu_c) = 0$$

$$\gamma_i^*(q_i^* - 1) = 0, \; i = 0, \ldots, n-1.$$

$$\gamma_n^*(R^* - \frac{\lambda_v - \sum_{i=1}^n \lambda_c^{(i)}}{n}) = 0.$$

$$\omega_i^* q_i^* = 0, \; i = 0, \ldots, n-1.$$

$$\omega_n^*(R^* - \epsilon_2) = 0.$$

$$\nu_{ij}^*(\Pi_{ij}^* - 1) = 0, \; i = 1, \ldots, n, \; j = 1, \ldots i.$$

$$\mu_{ij}^* \Pi_{ij}^* = 0, \; i = 1, \ldots, n, \; j = 1, \ldots i.$$

$$\delta_i^*(\sum_{j=1}^{i} \Pi_{ij}^* - 1) = 0, \; i = 1, \ldots, n. \tag{5.59}$$

Likewise, applying the KKT conditions to the Lagrangian function in (4.12), and knowing that the gradient of the Lagrangian function goes to 0 at the lower bound solution, we get

the following set of equalities:

$$\begin{aligned}
&\frac{\partial L}{\partial q_i} = \lambda_v p_i \left(\sum_{j=1}^{i} \alpha_j^* (\Pi_{i+1j}^* - \Pi_{ij}^*) + \alpha_{i+1}^* \Pi_{i+1i+1}^* - \beta_0^* \right) - \omega_i^* + \gamma_i^* = 0,\ i = 1, \ldots, n-1. \\
&\frac{\partial L}{\partial q_0} = \lambda_v p_0 \left(\alpha_1^* \Pi_{11}^* - \sum_{j=1}^{n} \alpha_j^* \Pi_{nj}^* - \beta_0^* + \beta_1^* \right) - \omega_0^* + \gamma_0^* = 0 \\
&\frac{\partial L}{\partial \Pi_{ij}} = \alpha_j^* \lambda_v \left(p_{i-1} {q_{i-1}}^* - p_{i-1} - p_i q_i^* \right) + \delta_i^* + \nu_{ij}^* - \mu_{ij}^* = 0 \\
&\frac{\partial L}{\partial \Pi_{nj}} = \alpha_j^* \lambda_v \left(p_{n-1} {q_{n-1}}^* - p_{n-1} - p_0 q_0^* \right) + \delta_n^* + \nu_{nj}^* - \mu_{nj}^* = 0 \\
&\frac{\partial L}{\partial R} = -1 + \sum_{i=1}^{n} \alpha_i^* - \omega_n^* + \gamma_n^* = 0
\end{aligned} \tag{5.60}$$

Multiplying the each of the partial derivatives in (5.60) by the derivation variable itself combined with the KKT conditions of the variables lower bounds inequalities given by (5.59) gives :

$$\begin{aligned}
&\frac{\partial L}{\partial q_i} \times q_i = q_i^* \lambda_v p_i \left(\sum_{j=1}^{i} \alpha_j^* (\Pi_{i+1j}^* - \Pi_{ij}^*) + \alpha_{i+1}^* \Pi_{i+1i+1}^* - \beta_0^* \right) + \gamma_i^* = 0,\ i = 1, \ldots, n-1. \\
&\frac{\partial L}{\partial q_0} \times q_0 = q_0^* \lambda_v p_0 \left(\alpha_1^* \Pi_{11}^* - \sum_{j=1}^{n} \alpha_j^* \Pi_{nj}^* - \beta_0^* + \beta_1^* \right) + \gamma_0^* = 0 \\
&\frac{\partial L}{\partial \Pi_{ij}} \times \Pi_{ij} = \Pi_{ij}^* \left(\alpha_j^* \lambda_v \left(p_{i-1} {q_{i-1}}^* - p_{i-1} - p_i q_i^* \right) + \delta_i^* \right) + \nu_{ij}^* = 0 \\
&\frac{\partial L}{\partial \Pi_{nj}} \times \Pi_{nj} = \Pi_{nj}^* \left(\alpha_j^* \lambda_v \left(p_{n-1} {q_{n-1}}^* - p_{n-1} - p_0 q_0^* \right) + \delta_n^* \right) + \nu_{nj}^* = 0 \\
&\frac{\partial L}{\partial R} \times R = -R + R \sum_{i=1}^{n} \alpha_i^* - \omega_n^* \epsilon_2 + \gamma_n^* \left(\frac{\lambda_v - \sum_{i=1}^{n} \lambda_c^{(i)}}{n} \right) = 0
\end{aligned} \tag{5.61}$$

When we inject the result of the first four equations in (5.61) in the KKT conditions on the upper bound conditions of the variables q_i and Π_{ij} we find:

$$\begin{aligned}
&q_i^*(q_i^*-1)\left(\sum_{j=1}^{i}\alpha_j^*(\Pi_{i+1j}^*-\Pi_{ij}^*)+\alpha_{i+1}^*\Pi_{i+1i+1}^*-\beta_0^*\right)=0,\ i=1,\ldots,n-1.\\
&q_0^*(q_0^*-1)\left(\alpha_1^*\Pi_{11}^*-\sum_{j=1}^{n}\alpha_j^*\Pi_{nj}^*-\beta_0^*+\beta_1^*\right)=0\\
&\Pi_{ij}^*(\Pi_{ij}^*-1)\left(\alpha_j^*\lambda_v\left(p_{i-1}{q_{i-1}}^*-p_{i-1}-p_iq_i^*\right)+\delta_i^*\right)=0\\
&\Pi_{nj}^*(\Pi_{nj}^*-1)\left(\alpha_j^*\lambda_v\left(p_{n-1}{q_{n-1}}^*-p_{n-1}-p_0q_0^*\right)+\delta_n^*\right)=0
\end{aligned}\tag{5.62}$$

From (5.62) we have :

$0<q_0^*<1$ only if $\alpha_1^*\Pi_{11}^*-\sum_{j=1}^{n}\alpha_j^*\Pi_{nj}^*-\beta_0^*+\beta_1^*=0$

$0<q_i^*<1$ only if $\sum_{j=1}^{i}\alpha_j^*(\Pi_{i+1j}^*-\Pi_{ij}^*)+\alpha_{i+1}^*\Pi_{i+1i+1}^*-\beta_0^*=0$

$0<\Pi_{ij}^*<1$ only if $\alpha_j^*\lambda_v\left(p_{i-1}{q_{i-1}}^*-p_{i-1}-p_iq_i^*\right)+\delta_i^*=0$

$0<\Pi_{nj}^*<1$ only if $\alpha_j^*\lambda_v\left(p_{n-1}{q_{n-1}}^*-p_{n-1}-p_0q_0^*\right)+\delta_n^*=0$

Since $0\leq q_i^*\leq 1$ and $0\leq\Pi_{ij}^*\leq 1$ then these equalities may not always be true

if $\alpha_1^*\Pi_{11}^*-\sum_{j=1}^{n}\alpha_j^*\Pi_{nj}^*-\beta_0^*+\beta_1^*>0$ and we know that $\gamma_0^*\geq 0$ then $\gamma_0^*=0$ which gives $q_0^*\neq 1$ and $q_0^*=0$.

if $\sum_{j=1}^{i}\alpha_j^*(\Pi_{i+1j}^*-\Pi_{ij}^*)+\alpha_{i+1}^*\Pi_{i+1i+1}^*-\beta_0^*>0$ which gives $q_i^*\neq 1$ and $q_i^*=0$

if $\alpha_1^*\Pi_{11}^*-\sum_{j=1}^{n}\alpha_j^*\Pi_{nj}^*-\beta_0^*+\beta_1^*<0$ then $\gamma_0^*>0$ (it cannot be 0 because this will contradict with the value of q_i), which implies that $q_0^*=1$.

if $\sum_{j=1}^{i}\alpha_j^*(\Pi_{i+1j}^*-\Pi_{ij}^*)+\alpha_{i+1}^*\Pi_{i+1i+1}^*-\beta_0^*<0$ then $\gamma_i^*>0$ (it cannot be 0 because this contradicts with the value of q_i), which implies that $q_i^*=1$

if $\alpha_j^*\lambda_v\left(p_{i-1}{q_{i-1}}^*-p_{i-1}-p_iq_i^*\right)+\delta_i^*>0$ and we know that $\nu_{ij}^*\geq 0$ then $\nu_{ij}^*=0$ which gives $\Pi_{ij}^*\neq 1$ and $\Pi_{ij}^*=0$.

if $\alpha_j^*\lambda_v\left(p_{n-1}{q_{n-1}}^*-p_{n-1}-p_0q_0^*\right)+\delta_n^*>0$ which gives $\Pi_{nj}^*\neq 1$ and $\Pi_{nj}^*=0$

if $\alpha_j^* \lambda_v \left(p_{i-1} {q_{i-1}}^* - p_{i-1} - p_i q_i^*\right) + \delta_i^* < 0$ then $\nu_{ij}^* > 0$ (it cannot be 0 because this will contradict with the value of Π_{ij}), which implies that $\Pi_{ij} = 1$.
if $\alpha_j^* \lambda_v \left(p_{n-1} {q_{n-1}}^* - p_{n-1} - p_0 q_0^*\right) + \delta_n^* < 0$ then $\nu_{nj}^* > 0$ (it cannot be 0 because this will contradict with the value of Π_{nj}), which implies that $\Pi_{nj} = 1$.

We have also from the KKT conditions given by equation in in (5.59) that says either the Lagrangian coefficient is 0 or its the associated inequality is an equality:
if $\beta_1^* \neq 0$ we have $q_0^* = \frac{\mu_c}{\lambda_v^* p_0}$
if $\alpha_n^* \neq 0$ we have $\frac{\lambda_c^{(n)} + \lambda_v p_{n-1} q_{n-1}^* \Pi_{nn}^* - \lambda_v p_{n-1} \Pi_{nn}^* + R^*}{\lambda_v p_0 \Pi n n^*}$
if $\alpha_i^* \neq 0$, we have $q_i^* = \frac{R^* + \lambda_c^{(i)} + \lambda_v \left[\sum_{k=i+2}^{n-1} (p_{k-1} q_{k-1}^* - p_k q_k^*) \Pi_{ki} + (p_{n-1} q_{n-1}^* - p_0 q_0^*) \Pi_{ni} - \sum_{k=i}^{n} p_{k-1} \Pi_{ki} + p_{i-1} q_{i-1}^* \Pi_{ii}^* - p_{i+1} q_{i+1} \Pi_{i}\right.}{\lambda_v p_i (\Pi_{ii} - \Pi_{i+1 i+1})}$
for $i = 1, \ldots, n-1$

Otherwise by the Lagrangian relaxation:
$q_i^* = \zeta_i(R^*, q^*, \Pi^*, \alpha^*, \beta^*, \gamma^*, \omega^*, \mu^*, \nu^*, \delta^*)$ for $i = 1, \ldots, n-1$ and $\Pi_{ij}^* = \zeta_{ij}(R^*, q^*, \Pi^*, \alpha^*, \beta^*, \gamma^*, \omega^*, \mu^*, \nu^*,$
where ζ_i and ζ_{ij} are the solution that that maximize $\inf_{\mathbf{q}, \mathbf{\Pi}} L(\mathbf{q}, \Pi^*, R^*, \alpha^*, \beta^*, \gamma^*, \omega^*, \mu^*, \nu^*, \delta^*)$

Now in order to find the expression of R^* we first look at its upper bound associated condition in (5.59). From there we can say that if $\omega_n^* \neq 0$ then $R^* = \epsilon_2$ and if $\gamma_n^* \neq 0$ then $R* = \frac{\lambda_v - \sum_{i=1}^{n} \lambda_c^{(i)}}{n}$

Otherwise, from the last equation in (5.61), if $\omega_n^* = 0$ and $\gamma_n^* = 0$ then

$$R^* = \sum_{i=1}^{n-1} \alpha_i^* (\lambda_v \sum_{k=i}^{n-1} (p_{k-1} - p_{k-1} q_{k-1}^* + p_k q_k^*) \Pi_{ki}^* + \lambda_v (p_{n-1} - p_{n-1} q_{n-1}^* + p_0 q_0^*) \Pi_{ni}^* - \lambda_c^{(i)})$$
$$+ \alpha_n^* (\lambda_v (p_{n-1} - p_{n-1} q_{n-1}^* + p_0 q_0^*) \Pi_{nn}^* - \lambda_c^{(n)}) \tag{5.63}$$

Appendix L: IEEE Copyright Permission